

# Supporting Information

## Chroman-4-one- and Chromone-based Sirtuin 2 Inhibitors with Antiproliferative Properties in Cancer Cells

Tina Seifert,<sup>†</sup> Marcus Malo,<sup>†</sup> Tarja Kokkola,<sup>‡</sup> Karin Engen,<sup>†</sup> Maria Fridén-Saxin,<sup>†</sup> Erik A. A. Wallén,<sup>§</sup> Maija Lahtela-Kakkonen,<sup>‡</sup> Elina M. Jarho,<sup>‡,\*</sup> Kristina Luthman<sup>†,\*</sup>

<sup>†</sup>Department of Chemistry and Molecular Biology, Medicinal Chemistry, University of Gothenburg, SE-412 96 Göteborg, Sweden, <sup>‡</sup>School of Pharmacy, Institute of Clinical Medicine, University of Eastern Finland, P.O. Box 1627, 70211 Kuopio, Finland, <sup>§</sup>Department of Pharmaceutical Chemistry, University of Helsinki, FIN-00014 Helsinki, Finland

### ***Table of Contents***

1	Elemental analyses.....	2
2	HRMS analysis .....	2
3	Results from SIRT1-3 assays.....	3
4	Physicochemical Properties .....	5
5	Homology Modeling.....	6
6	<sup>1</sup> H NMR and <sup>13</sup> C NMR spectra.....	10
7	References.....	48

## 1 Elemental analyses

**Table S1.** Data of combustion analyses for compounds **6a–i**, **10a–b**, **11a–c**, **11e**, **12a–b**, **17a–b**, **18a–b** and **21–24**.

Compd	Formula	Calculated			Analyzed		
		%C	%H	%N	%C	%H	%N
<b>6a</b>	C <sub>12</sub> H <sub>12</sub> BrClO <sub>3</sub>	45.10	3.78	0.00	45.15	3.71	0.03
<b>6b</b>	C <sub>13</sub> H <sub>14</sub> BrClO <sub>3</sub>	46.80	4.23	0.00	47.07	4.25	0.00
<b>6c</b>	C <sub>14</sub> H <sub>16</sub> BrClO <sub>3</sub>	48.37	4.64	0.00	48.56	4.65	0.00
<b>6d</b>	C <sub>13</sub> H <sub>14</sub> BrClO <sub>4</sub>	44.66	4.04	0.00	44.97	3.98	0.03
<b>6e</b>	C <sub>16</sub> H <sub>13</sub> BrClNO <sub>2</sub>	52.41	3.57	3.82	52.56	3.44	3.84
<b>6f</b>	C <sub>16</sub> H <sub>13</sub> BrClNO <sub>2</sub>	52.41	3.57	3.82	52.35	3.41	3.77
<b>6g</b>	C <sub>16</sub> H <sub>13</sub> BrClNO <sub>2</sub>	52.41	3.57	3.82	52.46	3.40	3.98
<b>6h</b>	C <sub>14</sub> H <sub>17</sub> BrO <sub>2</sub>	56.58	5.77	0.00	56.72	5.72	0.03
<b>6i</b>	C <sub>14</sub> H <sub>16</sub> BrClO <sub>2</sub>	50.70	4.86	0.00	51.42	4.86	0.21
<b>9a</b>	C <sub>13</sub> H <sub>12</sub> BrClO <sub>4</sub>	44.92	3.48	0.00	45.25	3.16	0.00
<b>9b</b>	C <sub>14</sub> H <sub>14</sub> BrClO <sub>4</sub>	46.50	3.90	0.00	46.64	3.80	0.03
<b>10a</b>	C <sub>12</sub> H <sub>10</sub> BrClO <sub>4</sub>	43.21	3.02	0.00	43.32	2.92	0.07
<b>10b</b>	C <sub>14</sub> H <sub>14</sub> BrClO <sub>4</sub>	44.92	3.48	0.00	44.89	3.46	0.01
<b>11a</b>	C <sub>13</sub> H <sub>13</sub> BrClNO <sub>3</sub>	45.05	3.78	4.04	45.33	3.75	3.92
<b>11b</b>	C <sub>14</sub> H <sub>15</sub> BrClNO <sub>3</sub>	46.63	4.19	3.88	47.28	4.23	3.78
<b>11c</b>	C <sub>16</sub> H <sub>19</sub> BrClNO <sub>3</sub>	49.44	4.93	3.60	49.82	4.93	3.53
<b>11e</b>	C <sub>15</sub> H <sub>17</sub> BrClNO <sub>3</sub>	48.09	4.57	3.74	48.15	4.63	3.59
<b>12a</b>	C <sub>14</sub> H <sub>12</sub> BrClNO <sub>3</sub>	45.25	3.25	7.54	45.54	3.08	7.45
<b>12b</b>	C <sub>15</sub> H <sub>14</sub> BrClNO <sub>3</sub>	46.72	3.66	7.26	47.10	3.51	7.14
<b>17a</b>	C <sub>16</sub> H <sub>19</sub> BrClNO <sub>3</sub>	49.44	4.93	3.60	49.04	4.76	3.55
<b>17b</b>	C <sub>17</sub> H <sub>21</sub> BrClNO <sub>2</sub>	52.80	5.47	3.62	52.70	5.51	3.45
<b>20b</b>	C <sub>20</sub> H <sub>15</sub> BrClNO <sub>2</sub> ×0.3 H <sub>2</sub> O	56.91	3.58	3.32	56.72	3.94	3.02
<b>22</b>	C <sub>19</sub> H <sub>15</sub> BrClNO <sub>3</sub>	53.92	3.46	3.70	53.51	3.36	3.49
<b>23</b>	C <sub>19</sub> H <sub>15</sub> BrClNO <sub>3</sub>	54.25	3.59	3.33	54.24	3.44	3.20
<b>24</b>	C <sub>18</sub> H <sub>11</sub> BrClNO <sub>2</sub>	55.63	2.85	3.60	55.77	2.63	3.51

## 2 HRMS analysis

**Table S2.** Data of HRMS analyses.

Compd	Formula	Mass <sup>a</sup>		purity <sup>b</sup> (%)
		Calcd	Found	
<b>11d</b>	C <sub>20</sub> H <sub>19</sub> BrClNO <sub>3</sub>	436.0315	436.0315	98
<b>20a</b>	C <sub>20</sub> H <sub>15</sub> BrClNO <sub>3</sub>	432.0002	432.0025	95

<sup>a</sup>ESI<sup>+</sup>, LCTP, Acquity UPLC BEH C18, 2.1 mm×50 mm, 1.7 μm particles, 50 °C, 2–95% MeCN, 3 min, pH 10, <sup>b</sup>Relative Absorbance at 210 nm.

### 3 Results from SIRT1-3 assays

**Table S3.** SIRT1–3 activity assay results.

No.	$\text{R}^2$	$\text{R}^3$	$\text{R}^6$	$\text{R}^8$	Inhibition $\pm$ SD at 200 $\mu\text{M}$ (%) <sup>a</sup>			SIRT2 $\text{IC}_{50}$ ( $\mu\text{M}$ ) <sup>b,c</sup>
					SIRT1	SIRT2	SIRT3	
1		H	Cl	Br	6.2 $\pm$ 1.4	88 $\pm$ 0.9	2.6 $\pm$ 1.3	4.3 (3.5–5.4)
2		H	Cl	Br	6.9 $\pm$ 3.4	81 $\pm$ 0.7	16 $\pm$ 0.9	6.8 (5.8–8.0)
6a		H	Cl	Br	n.d.	18 $\pm$ 1.1	n.d.	n.d.
6b		H	Cl	Br	n.d.	52 $\pm$ 0.9	n.d.	n.d.
6c		H	Cl	Br	n.d.	67 $\pm$ 0.5	n.d.	n.d.
6d		H	Cl	Br	n.d.	33 $\pm$ 2.0	n.d.	n.d.
6e		H	Cl	Br	23 $\pm$ 2.1	74 $\pm$ 0.5	32 $\pm$ 1.1	n.d.
6f		H	Cl	Br	9.8 $\pm$ 0.9	86 $\pm$ 1.9	28 $\pm$ 0.8	3.7 (3.1–4.5)
6g		H	Cl	Br	23 $\pm$ 2.1	73 $\pm$ 1.8	32 $\pm$ 1.1	n.d.
6h		H	Br	H	n.d.	69 $\pm$ 1.2	n.d.	n.d.
6i		H	Br	Cl	3.8 $\pm$ 1.1	96 $\pm$ 2.8	6.4 $\pm$ 2.5	1.8 (1.5–2.0)
9a		H	Cl	Br	1.6 $\pm$ 1.9	80 $\pm$ 4.4	6.8 $\pm$ 2.2	9.6 (6.8–13.6)
9b		H	Cl	Br	4.8 $\pm$ 1.4	90 $\pm$ 0.5	15 $\pm$ 0.01	2.0 (1.6–2.5)
10a		H	Cl	Br	n.d.	6.8 $\pm$ 1.5	n.d.	n.d.
10b		H	Cl	Br	n.d.	7.6 $\pm$ 1.6	n.d.	n.d.
11a		H	Cl	Br	n.d.	4.8 $\pm$ 0.2	n.d.	n.d.

<b>11b</b>		H	Cl	Br	n.d.	$39 \pm 0.9$	n.d.	n.d.
<b>11c</b>		H	Cl	Br	n.d.	$23 \pm 1.8$	n.d.	n.d.
<b>11d</b>		H	Cl	Br	n.d.	$39 \pm 0.9$	n.d.	n.d.
<b>11e</b>		H	Cl	Br	n.d.	$53 \pm 1.4$	n.d.	n.d.
<b>12a</b>		H	Cl	Br	$6.7 \pm 0.9$	$77 \pm 0.8$	$13 \pm 2.2$	$12.2$ (10.2–14.7)
<b>12b</b>		H	Cl	Br	n.d.	$49 \pm 1.2$	n.d.	n.d.
<b>17a</b>		H	Cl	Br	n.d.	$17 \pm 10.7^d$	n.d.	n.d.
<b>17b</b>		H	Cl	Br	n.d.	$40 \pm 2.8^d$	n.d.	n.d.
<b>20a</b>		H	Cl	Br	n.d.	$59 \pm 1.0$	n.d.	n.d.
<b>20b</b>		H	Cl	Br	n.d.	$56 \pm 1.1$	n.d.	n.d.
<b>22</b>		NH <sub>2</sub>	Cl	Br	n.d.	$79 \pm 1.5$	n.d.	n.d.
<b>23</b>		NHAc	Cl	Br	$9.1 \pm 0.2$	$81 \pm 0.9$	$38 \pm 2.1$	$28.7$ (21.4–38.5)
<b>24</b>		CN	Cl	Br	n.d.	$50 \pm 1.0$	n.d.	n.d.
<b>25</b>			Cl	Br	n.d.	$76 \pm 1.9$	n.d.	n.d.

<sup>a</sup>SD, standard deviation (n = 3). <sup>b</sup>IC<sub>50</sub> (95% confidence interval). IC<sub>50</sub> values were determined for compounds showing  $\geq 80\%$  inhibition of SIRT2 at 200  $\mu\text{M}$  concentration or compounds evaluated in the cell proliferation assay. <sup>c</sup>n.d.= not determined. <sup>d</sup>SIRTAinty assay was used for the determination.

#### 4 Physicochemical Properties

**Table S4.** Data of calculated physicochemical properties of chroman-4-one and chromone derivatives.

No.	MW	ACDlogP	ACDlogD pH 7.4	PSA (Å <sup>2</sup> )	HBD <sup>a</sup>	HBA <sup>b</sup>
<b>1</b>	331.6	5.60	5.60	27.4	0	2
<b>2</b>	365.7	5.57	5.57	27.4	0	2
<b>6a</b>	319.6	2.86	2.86	49.9	1	3
<b>6b</b>	333.6	3.19	3.19	49.9	1	3
<b>6c</b>	347.6	3.70	3.70	49.9	1	3
<b>6d</b>	349.6	2.73	2.73	45.0	0	4
<b>6e</b>	366.6	3.84	3.84	37.6	0	3
<b>6f</b>	366.6	4.19	4.18	37.6	0	3
<b>6g</b>	366.6	4.18	4.16	37.6	0	3
<b>6h</b>	297.2	5.14	5.14	27.4	0	2
<b>6i</b>	331.6	5.98	5.98	27.4	0	2
<b>9a</b>	347.6	3.36	3.36	54.4	0	4
<b>9b</b>	361.6	3.77	3.77	54.4	0	4
<b>10a</b>	333.6	2.89	-0.04	68.2	1	4
<b>10b</b>	347.6	3.22	0.52	68.2	1	4
<b>11a</b>	346.6	2.53	2.53	60.2	1	4
<b>11b</b>	360.6	2.84	2.84	60.2	1	4
<b>11c</b>	388.7	3.71	3.71	60.2	1	4
<b>11d</b>	436.7	4.51	4.51	60.2	1	4
<b>11e</b>	374.7	3.24	3.24	46.8	0	4
<b>12a</b>	371.6	3.69	3.69	61.0	0	5
<b>12b</b>	385.6	4.18	4.18	61.0	0	5
<b>17a</b>	388.7	3.16	2.88	37.3	0	4
<b>17b</b>	386.7	4.74	2.58	28.6	0	3
<b>20a</b>	432.7	4.84	4.84	59.6	1	4
<b>20</b>	416.7	5.28	5.28	37.6	0	3
<b>22</b>	378.7	3.93	3.93	55.4	2	3
<b>23</b>	420.7	3.73	3.73	60.2	1	4
<b>24</b>	388.6	4.48	4.48	46.4	0	3
<b>25</b>	392.7	2.96	2.96	55.4	2	3

<sup>a</sup>Number of hydrogen bond donors. <sup>b</sup>Number of hydrogen bond acceptors

## 5 Homology Modeling

### Homology modeling of human SIRT2

As described in the main text the SIRT1/NAD<sup>+</sup>(S)-**37** complex (PDB code 4I5I)<sup>1</sup> was chosen as template for the homology modeling of human SIRT2. The homology modeling was performed using the MOE software (v. 2012.10, Chemical Computing Group Inc.: Montreal).

A multiple sequence alignment was performed in ClustalW (v. 2.1)<sup>2</sup> using the template (SIRT1 human, 4I5I (**Q96EB6**)), the main target (SIRT2 human, **Q8IXJ6**) and the human SIRT3 sequence (**Q9NTG7**). The result was fine-tuned to improve the final homology model (Figure S1). The force field used in the homology modeling in this study was Amber12:EHF with R-Field solvation, as implemented in the MOE software.

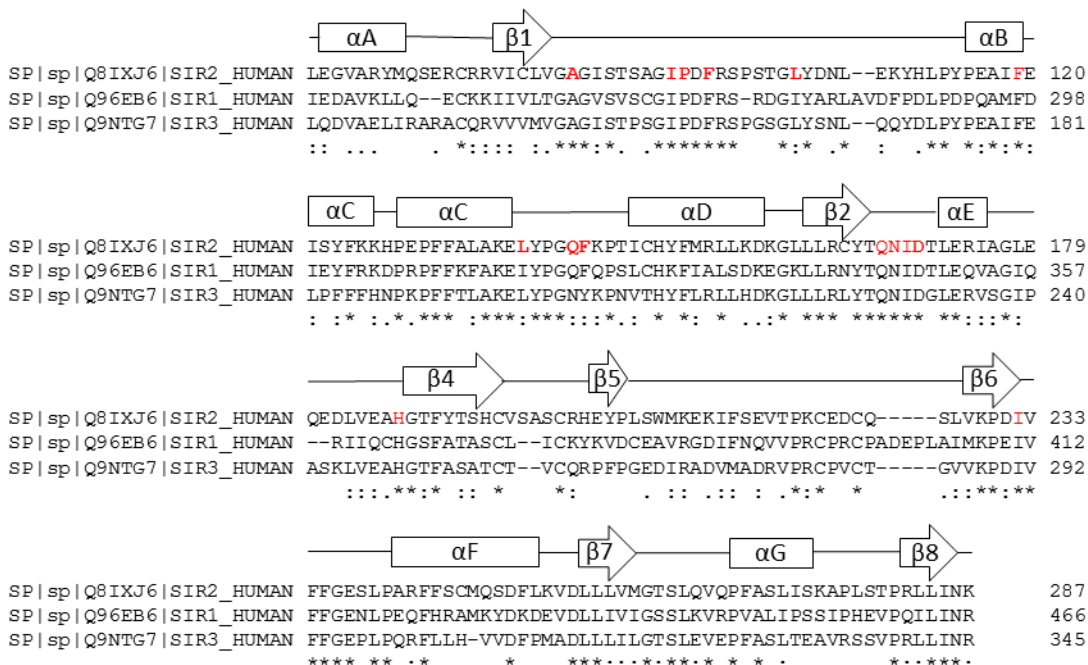


**Figure S1.** The final alignment of the human SIRT1–3 enzyme sequences (with amino acid sequence entries Q96EB6, Q8IXJ6 and Q9NTG7 respectively). The rectangles indicate the  $\alpha$ -helices and the arrows  $\beta$ -strands. The red marked amino acids are within 5 Å from the ligand in the SIRT2/6f-complex. The sequences were cut in both terminals as they differ in sequence identity, length and structure. These differences do not influence the amino acids involved in ligand binding in the C-pocket.

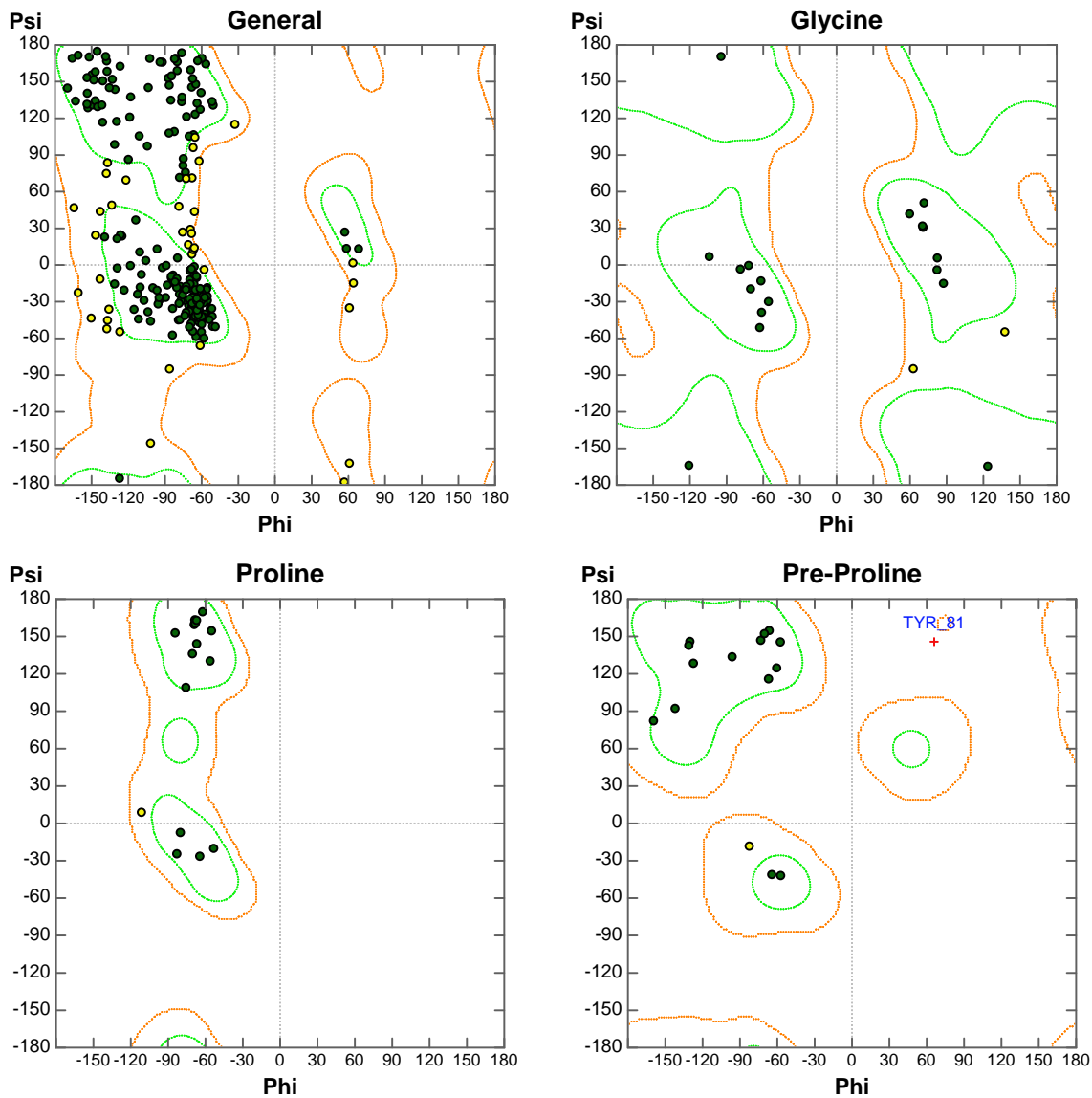
In the applied homology modelling procedure, all heavy atom positions of strictly conserved residues in the target model inherit their coordinates from the template. In non-conserved regions the backbone geometry was copied. Non-aligned regions where the backbone coordinates were not defined (i.e. regions with deletions or insertions that are often located in

loops) were modelled based on fragments from high-resolution regions of proteins in the Protein Data Bank<sup>3</sup> (PDB).<sup>4</sup> The fragment search included a clustering algorithm, which is based on similarity of the anchoring regions (each fragment consists of two anchor regions and a central region). The fragments were anchored to initially modelled residues and a contact energy function was used to rank fragment candidates, taking into account all atoms from conserved residues and any specified environment atoms. The coordinates for the chosen fragment structure were then copied to the homology model. Once all the loop structures had been selected, the side chains of the non-conserved residues were constructed. Side chains were modelled from data assembled from an extensive rotamer library generated by systematic clustering of high-resolution PDB data. A deterministic procedure based on unary quadratic optimization (UQO) was then run to select an optimal packing.<sup>5</sup> After all backbone segments and side chain conformations had been chosen for an intermediate model, hydrogen atoms were added to complete the valence requirements. The model was then submitted to a series of energy minimizations before the final preparation of the model was scored and written to an output database. The number of main chain models to be generated was specified in the program. In addition, structures with variations in the side chain conformations were generated for each model, however the first side chain model was always built using the UQO procedure. It is possible to specify molecules to be included as “environment” in the modeling procedure and these will be considered during the energy minimization stages.

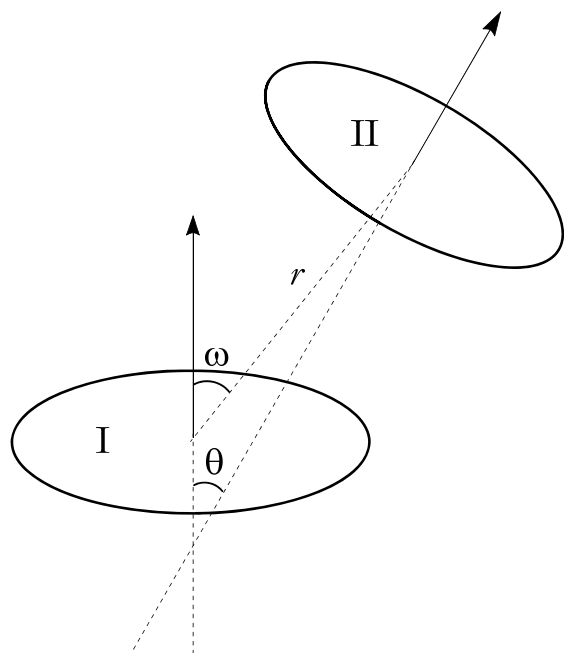
During the construction of the homology model inhibitor **6f** was included as environment and positioned in the C-pocket close to the location of **37** in the SIRT1 structure, in order to achieve more information regarding the inhibitor-enzyme interactions. NAD<sup>+</sup> was included in the modeling procedure with its position kept from the SIRT1 structure,<sup>1</sup> i.e. in its non-productive mode. Also the lysine residue from a Sir2-p53 peptide-NAD<sup>+</sup>-complex (2H4F) was included,<sup>6</sup> as were five structural water molecules from the SIRT1 structure (4I5I) positioned within 5 Å from the inhibitor (W2, W5, W17, W74, W78). The position of W17 seems to be present also in other sirtuins.<sup>7,8</sup>

During the modeling procedure, twenty homology models were generated independently and for each model all side-chain conformations were sampled three times, which makes it a total number of 60 models. The ensemble of models was scored based on geometrical quality and an energy minimization scheme was applied to the highest scored model. To refine the model, hydrogen atoms were added to the ligand, and the ionization and tautomeric states of the ligand–enzyme complex were determined.

The selected inhibitor-induced SIRT2 homology model showed good geometrical properties. The following protein structural properties were evaluated: 1) the bond lengths, angles and dihedrals of the protein backbone; 2) Ramachandran plots of  $\varphi$  and  $\psi$  dihedrals (general, glycine, proline, and pre-proline; for explanations see Figure S2); 3) side chain rotamer quality; and 4) non-bonded amino acid steric clashes.

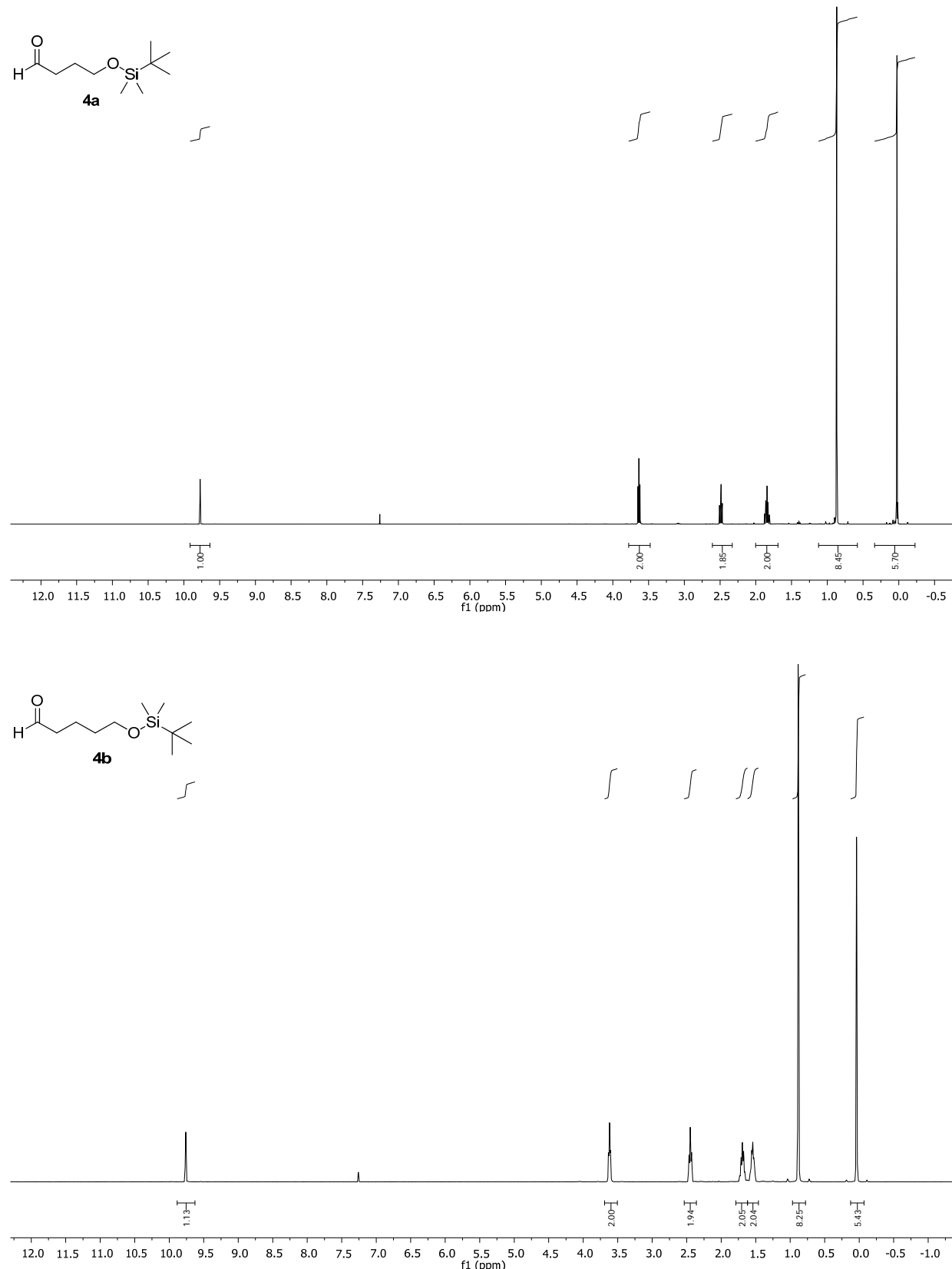


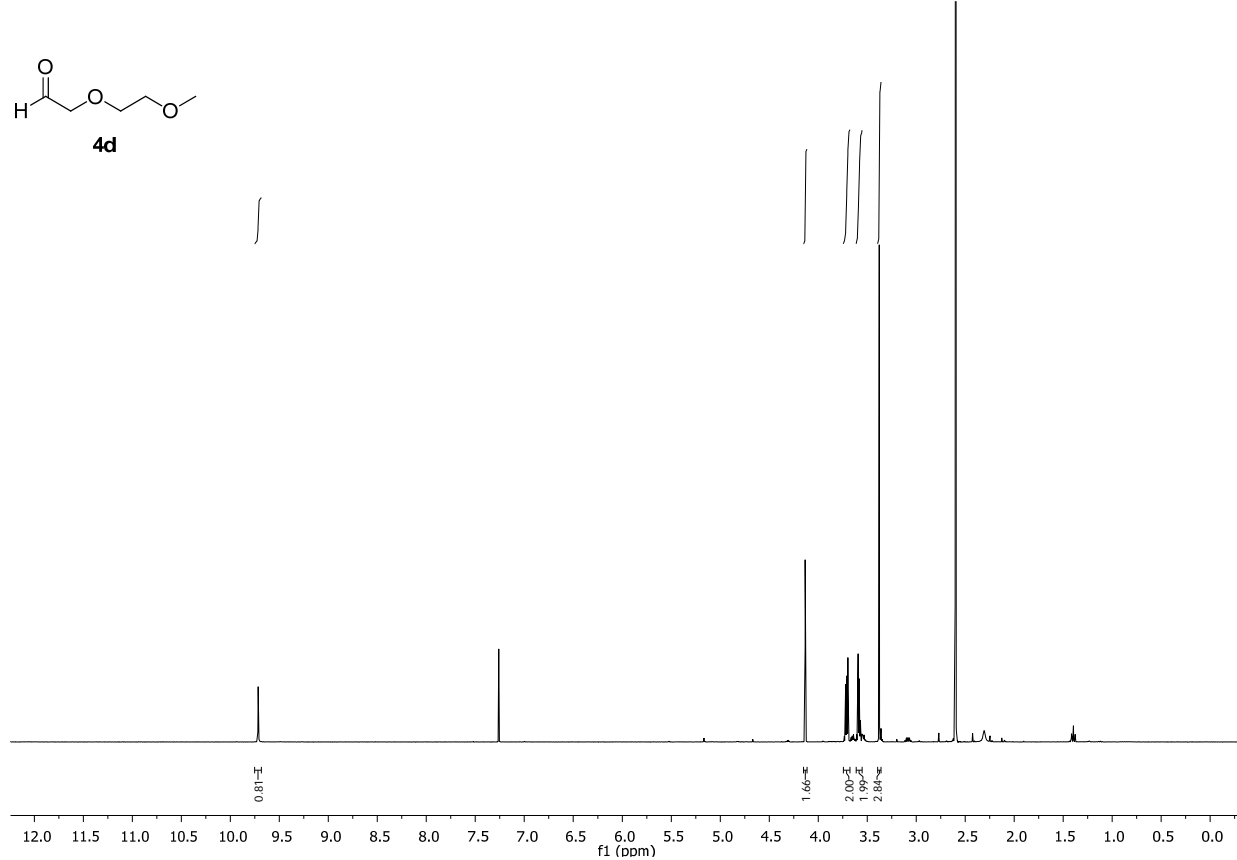
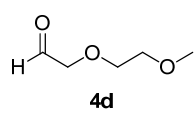
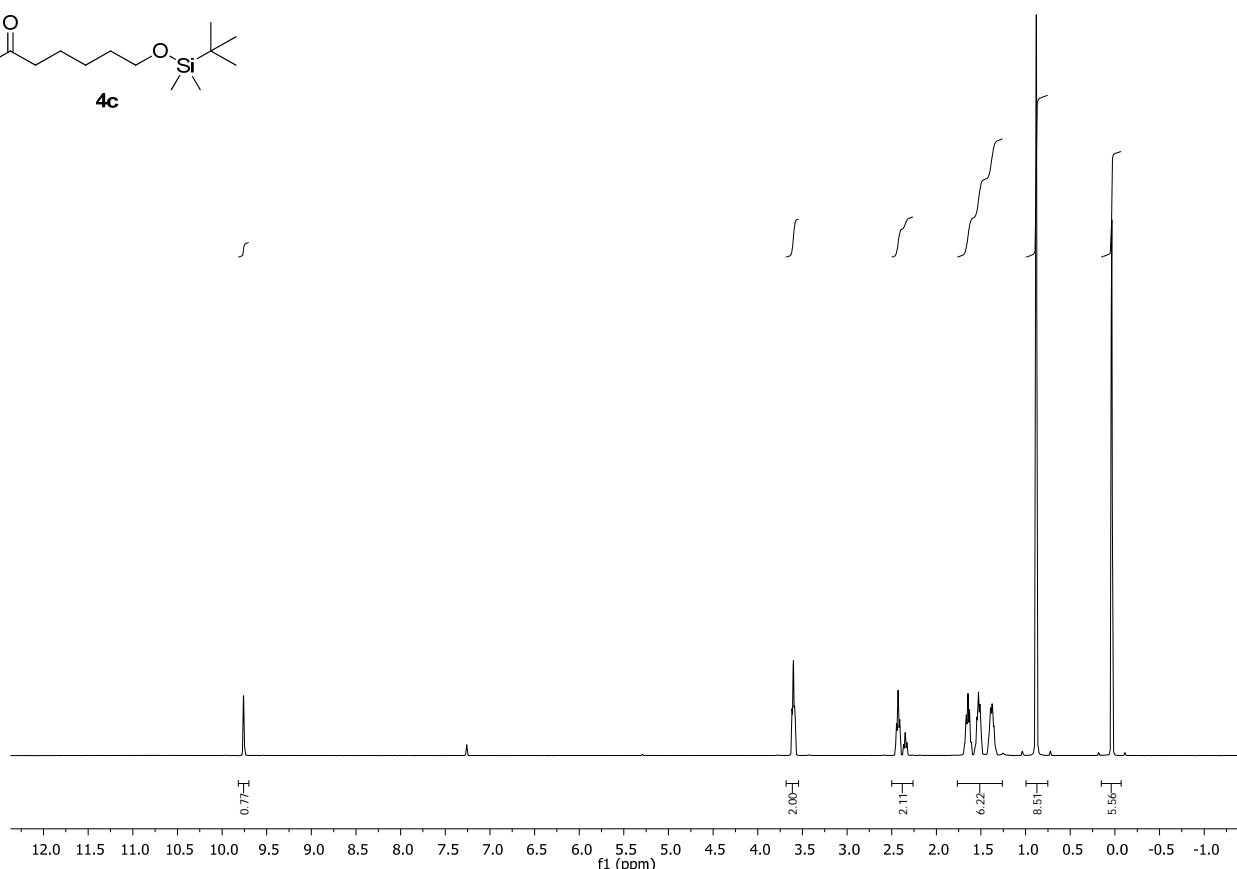
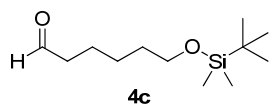
**Figure S2.** Ramachandran plots for glycine, proline, pre-proline and for general residues of the selected human SIRT2 homology model. The contours indicate allowed (orange) and core (green) regions of  $\varphi$  and  $\psi$  angles. A red cross indicates outliers. The outlier Tyr81 in the pre-proline plot is located approximately 15 Å from the inhibitor and the geometry are therefore, considered to be acceptable.

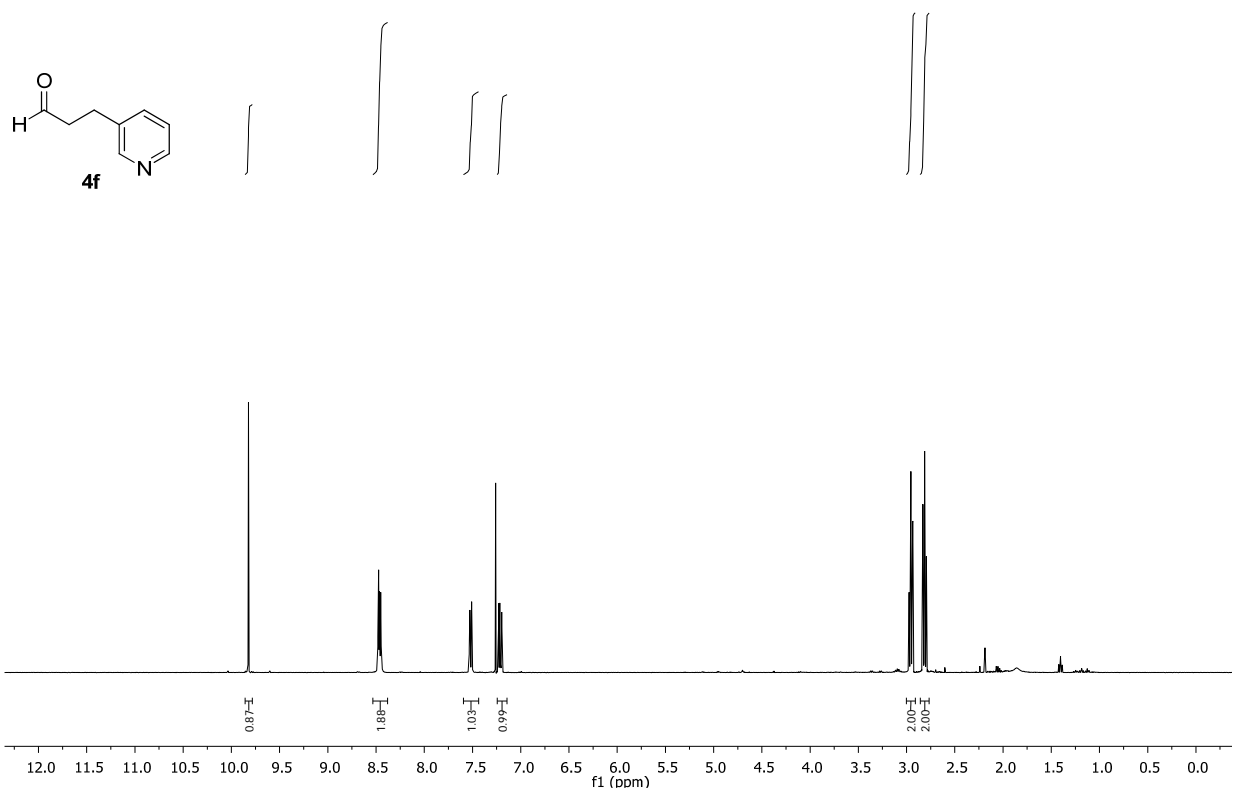
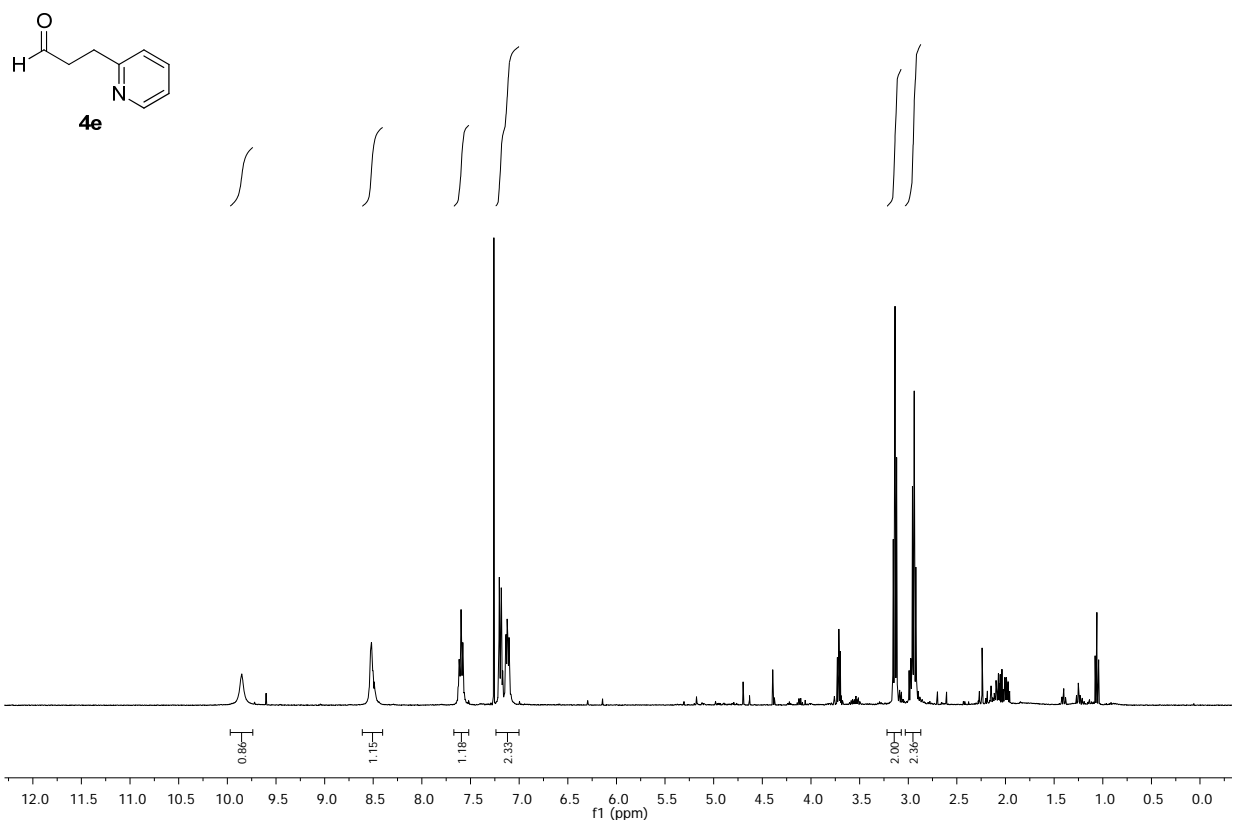


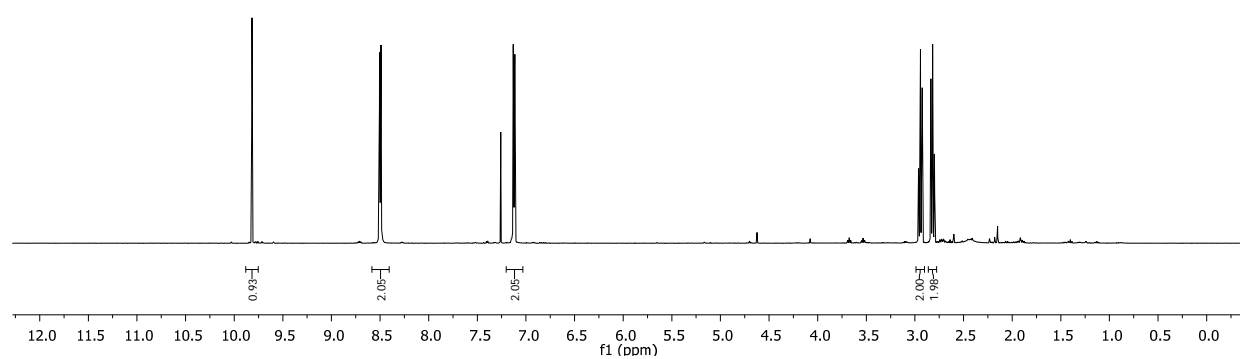
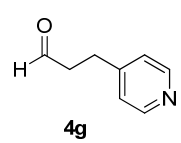
**Figure S5.** Coordinates defining the orientation of two planar moieties, I and II, e.g. two aromatic rings.  $\theta$  defines the angle between the normals of each plane and  $\omega$  defines the angle between the normal of ring I and the vector  $r$ , which connect the centroids of I and II. For a face-to-edge orientation of the aromatic rings, the distances ( $r$ ) should be between 4.5 and 5.5 Å, the  $\theta$ -angle between 75° and 90° and the  $\omega$  up to 15°. In the parallel displacement orientation,  $r$  should be between 3.5 and 4.5 Å and  $\theta$  up to 15° and  $\omega$  up to 30°.

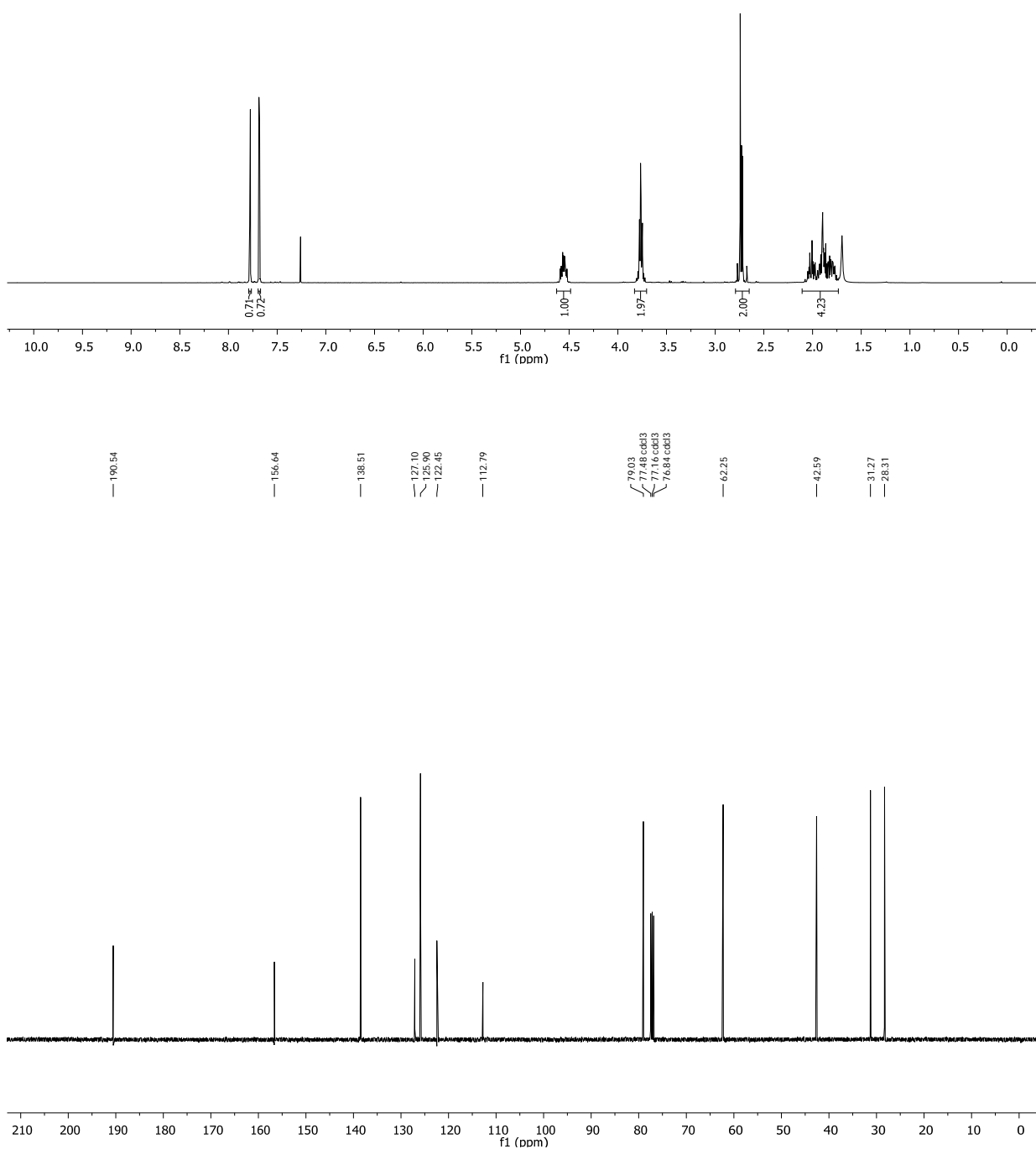
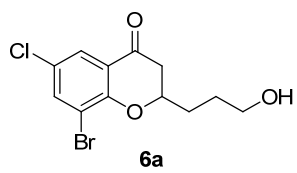
**6  $^1\text{H}$  NMR and  $^{13}\text{C}$  NMR spectra**

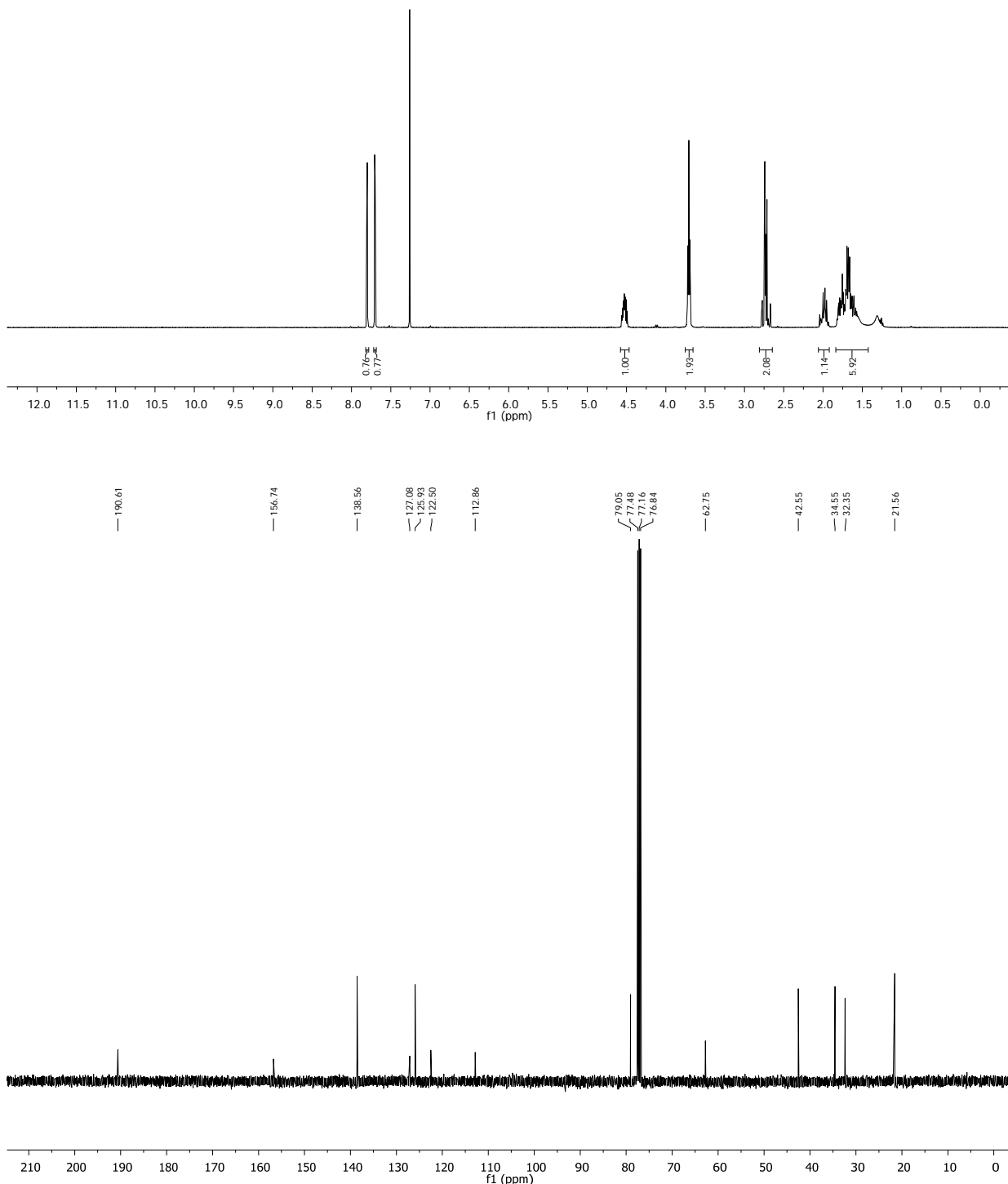
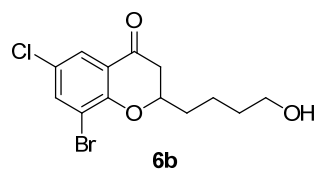


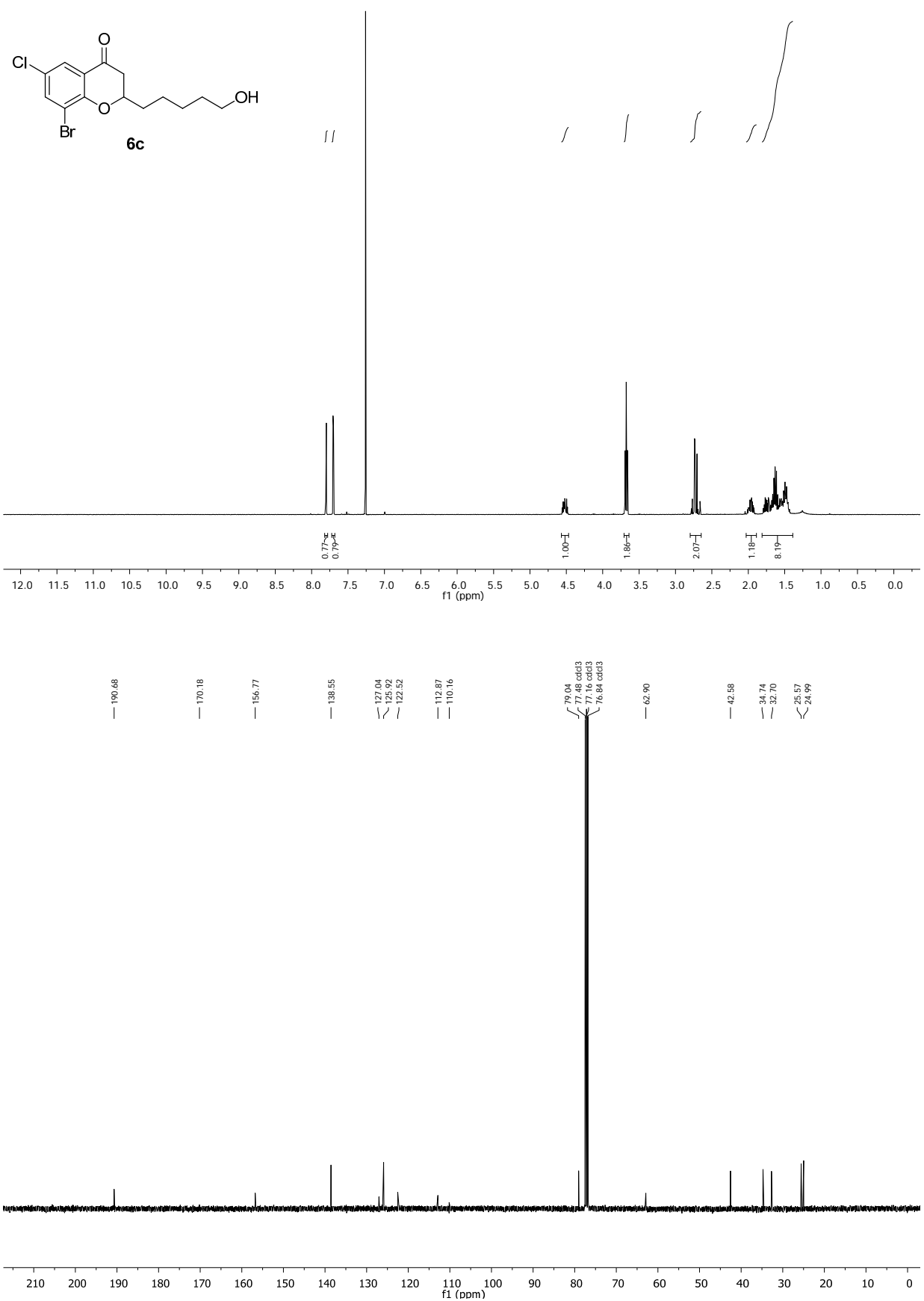


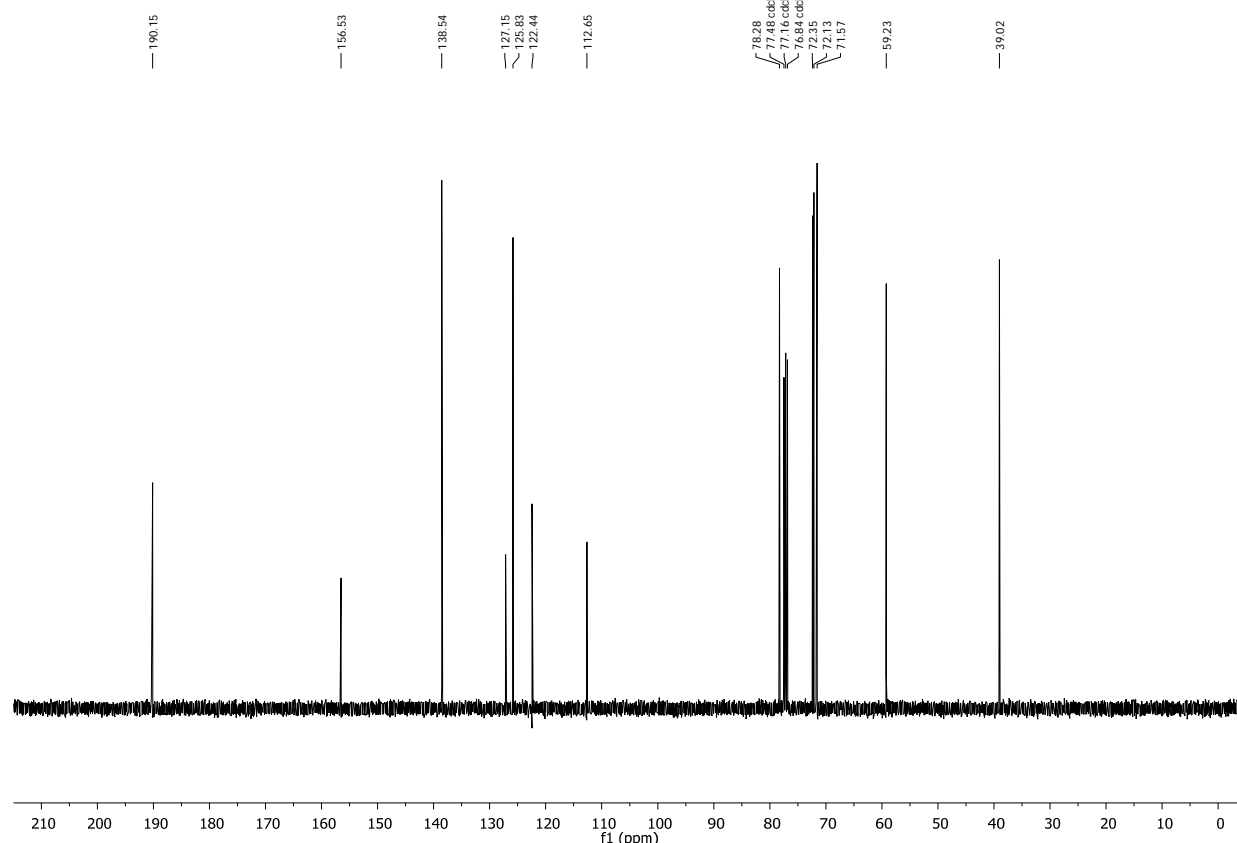
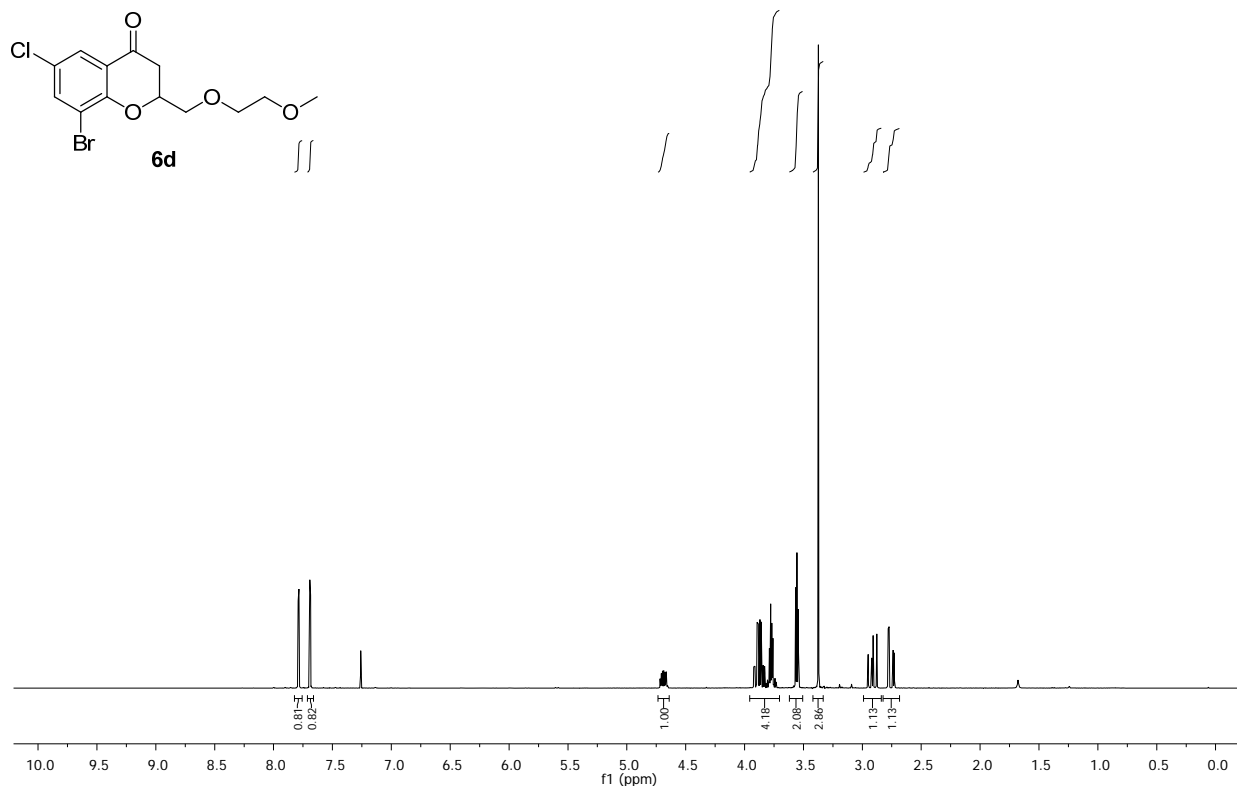


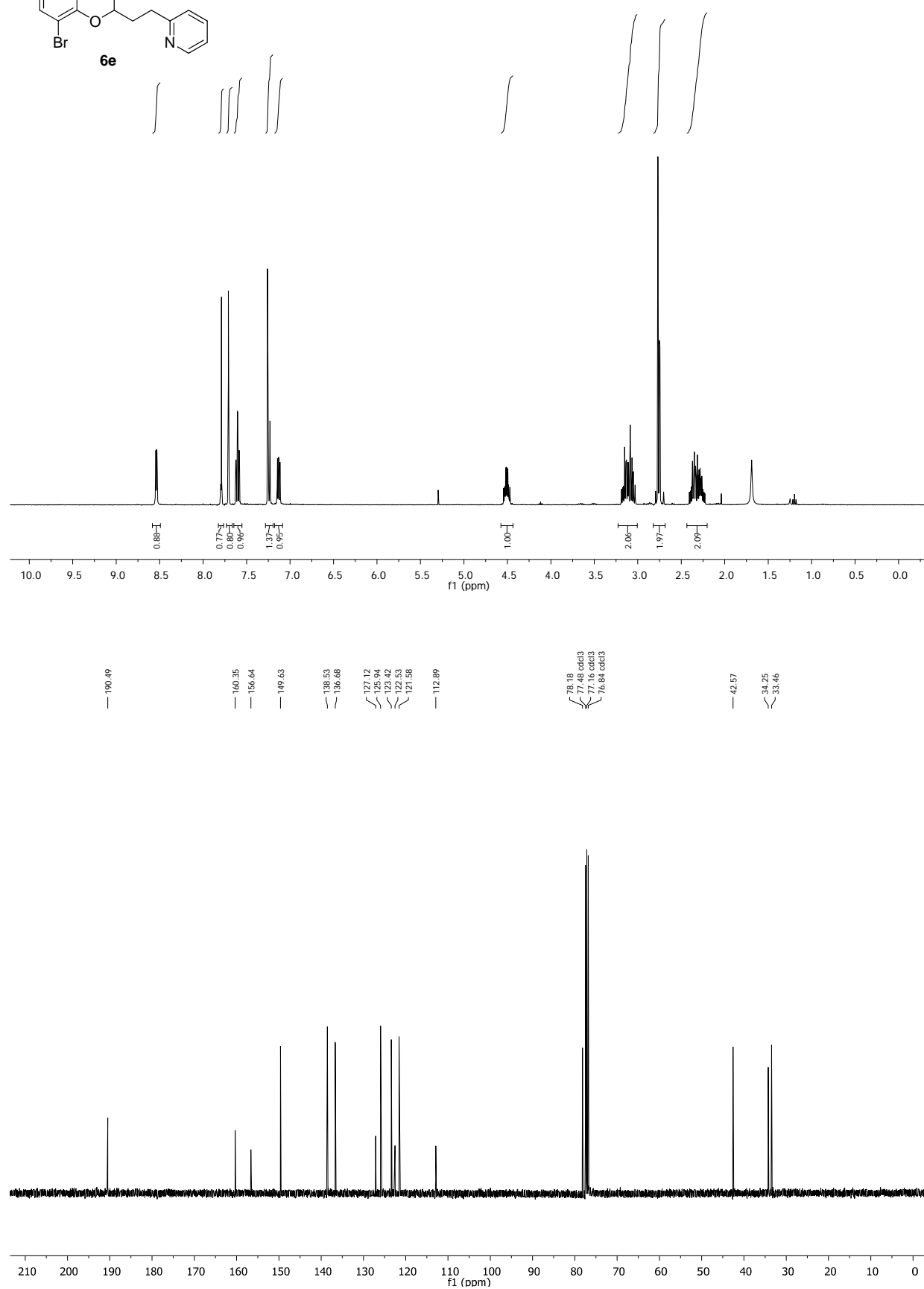
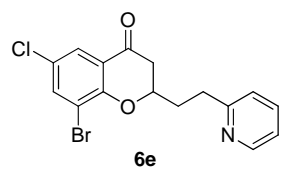


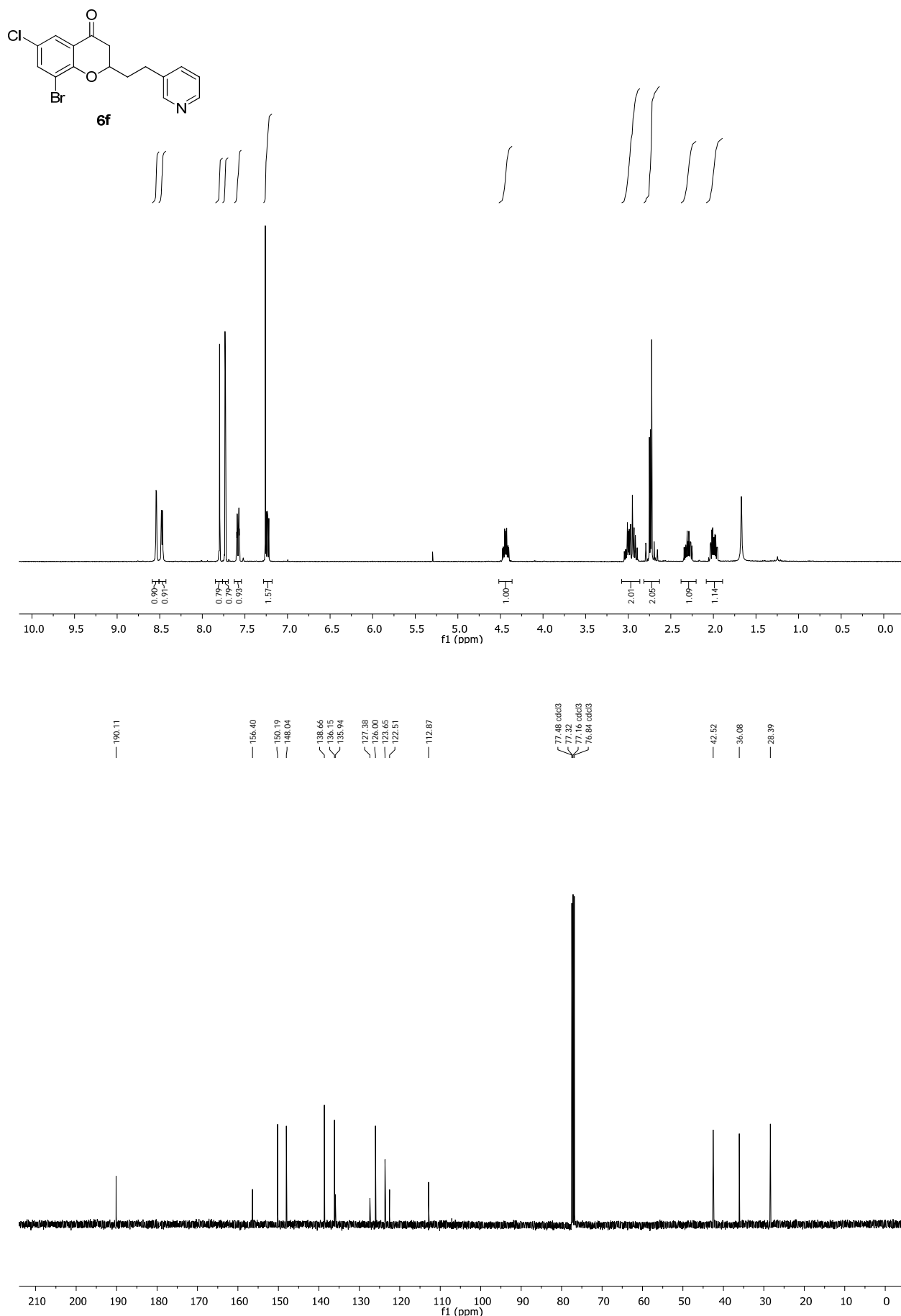


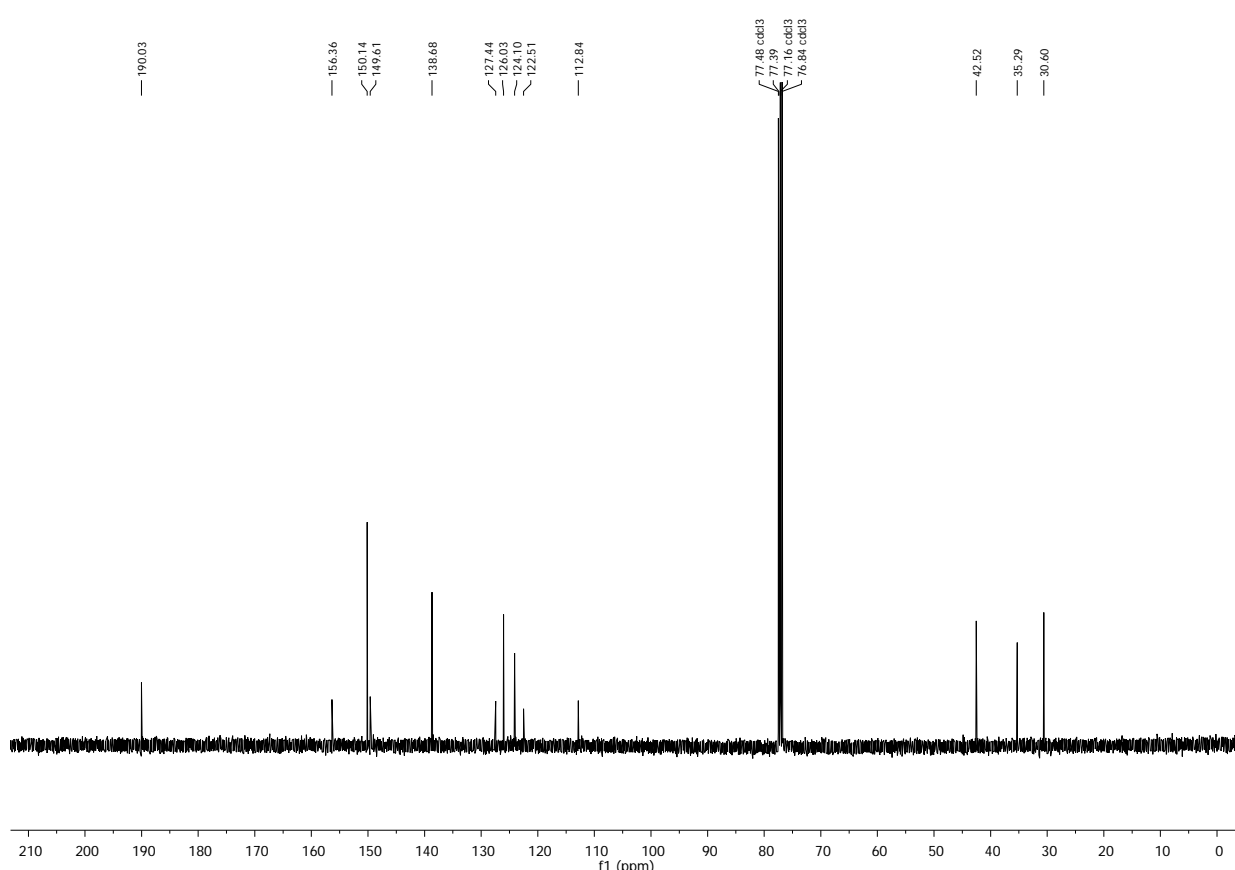
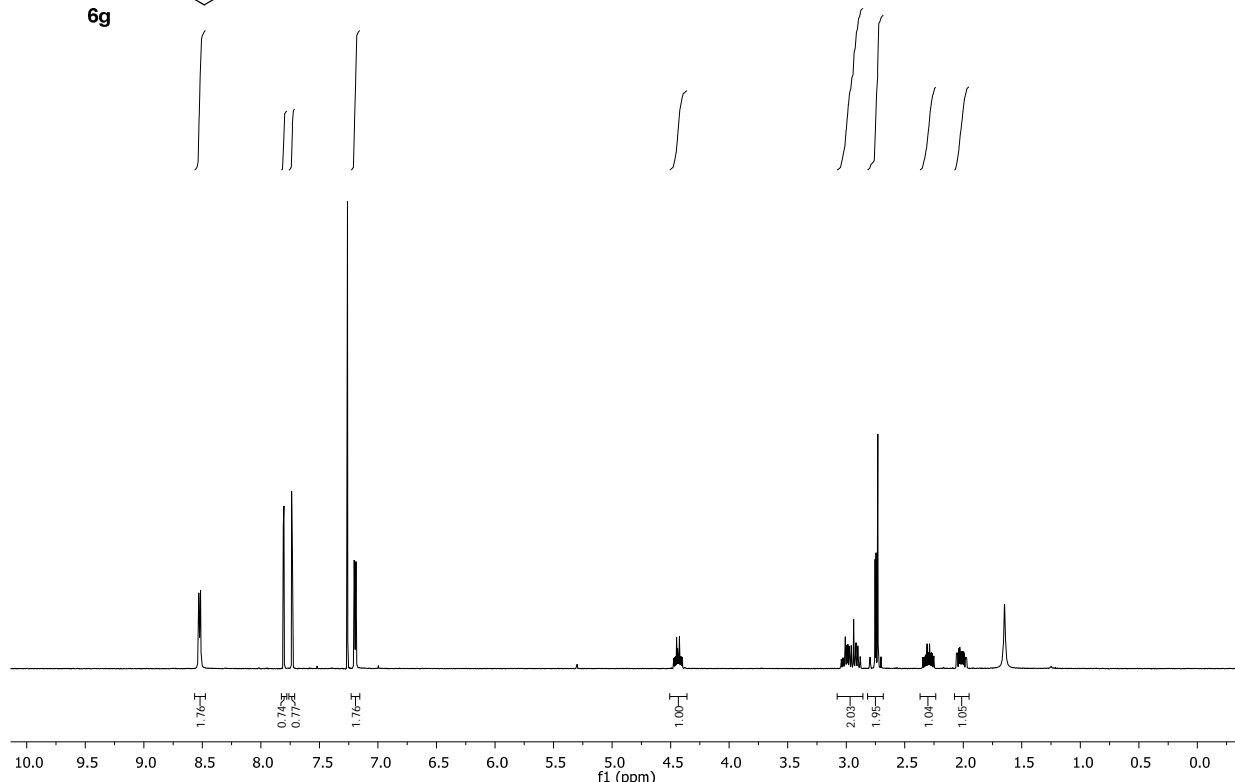
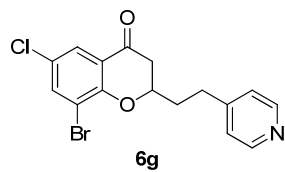


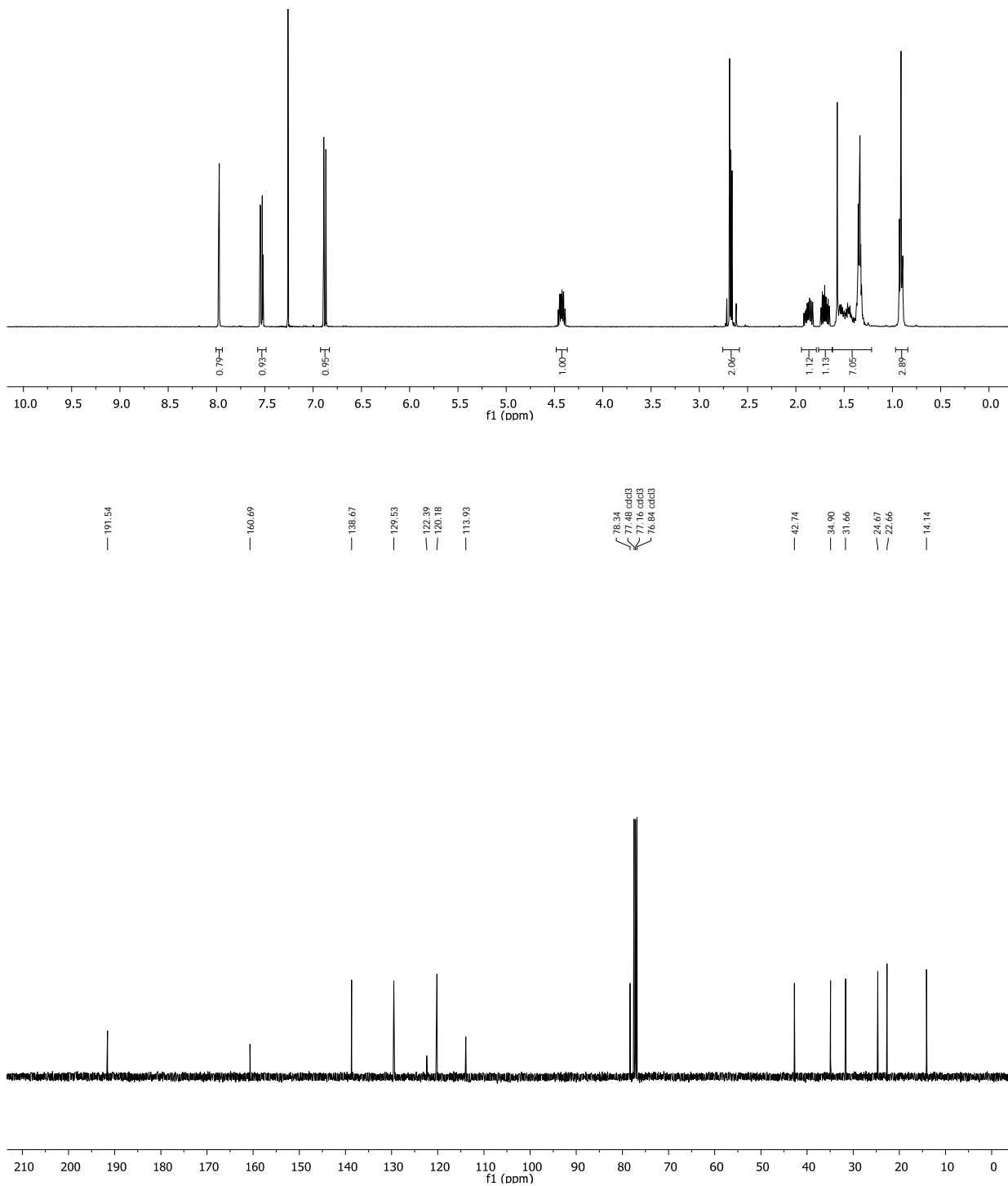
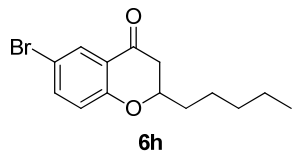


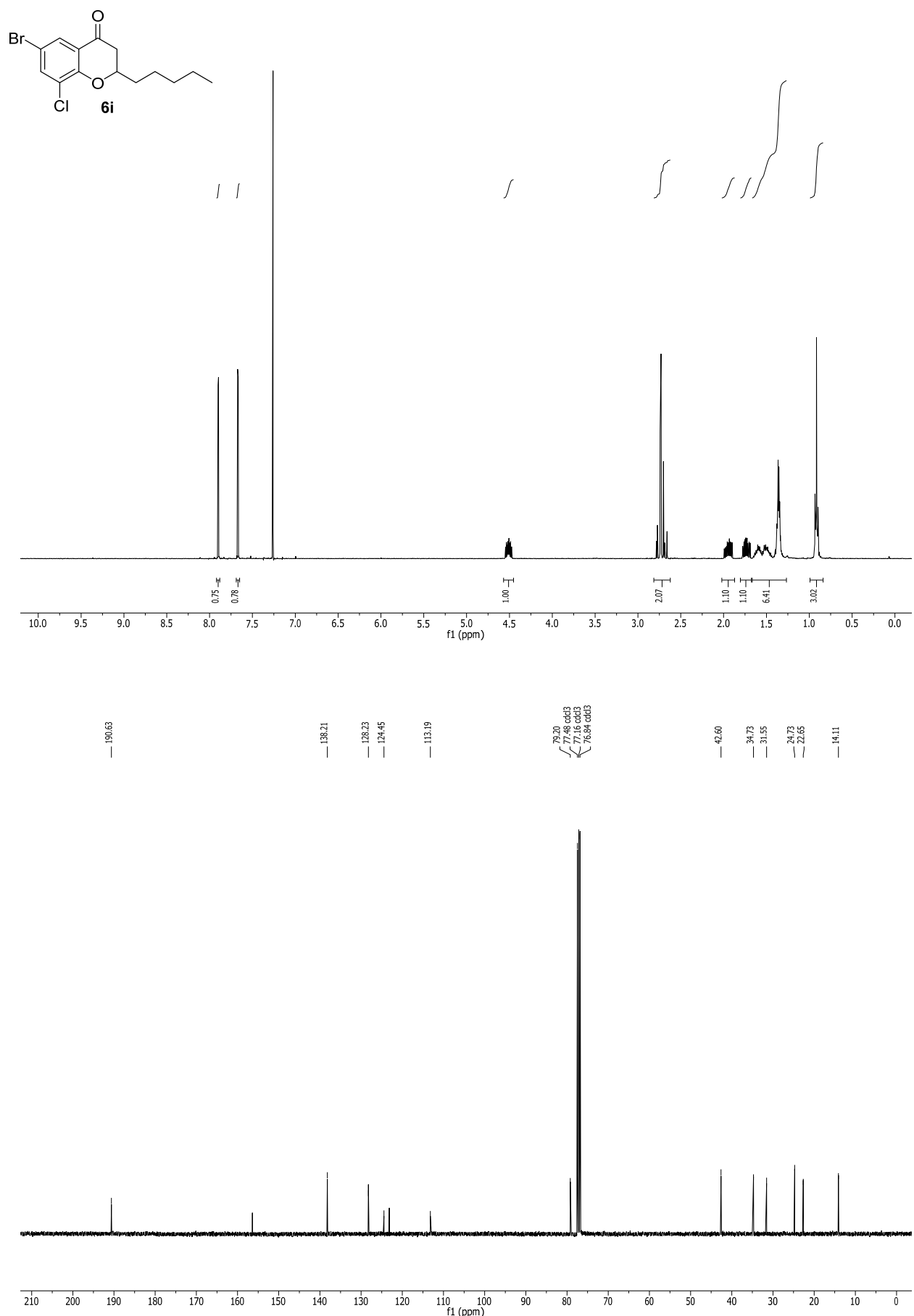


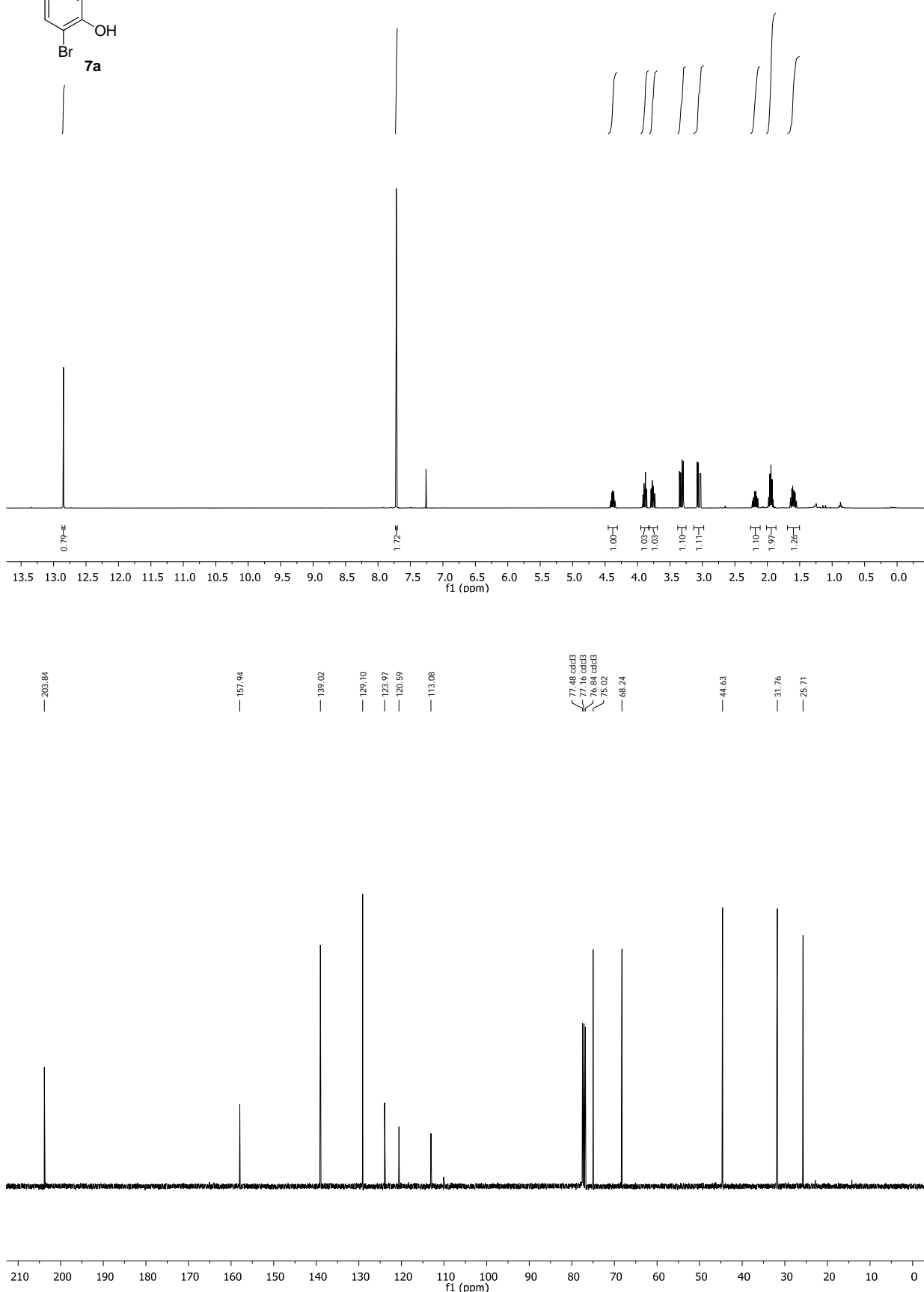
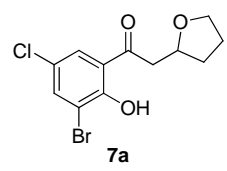


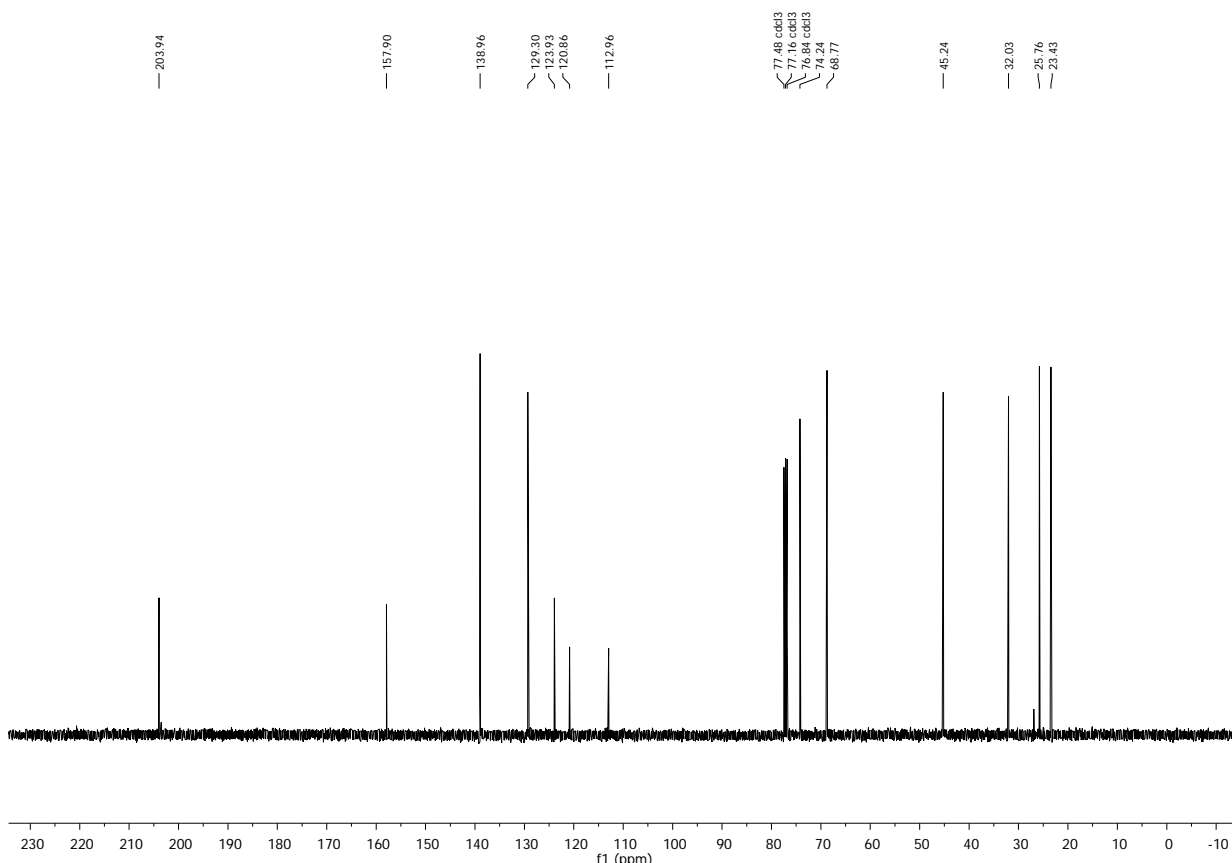
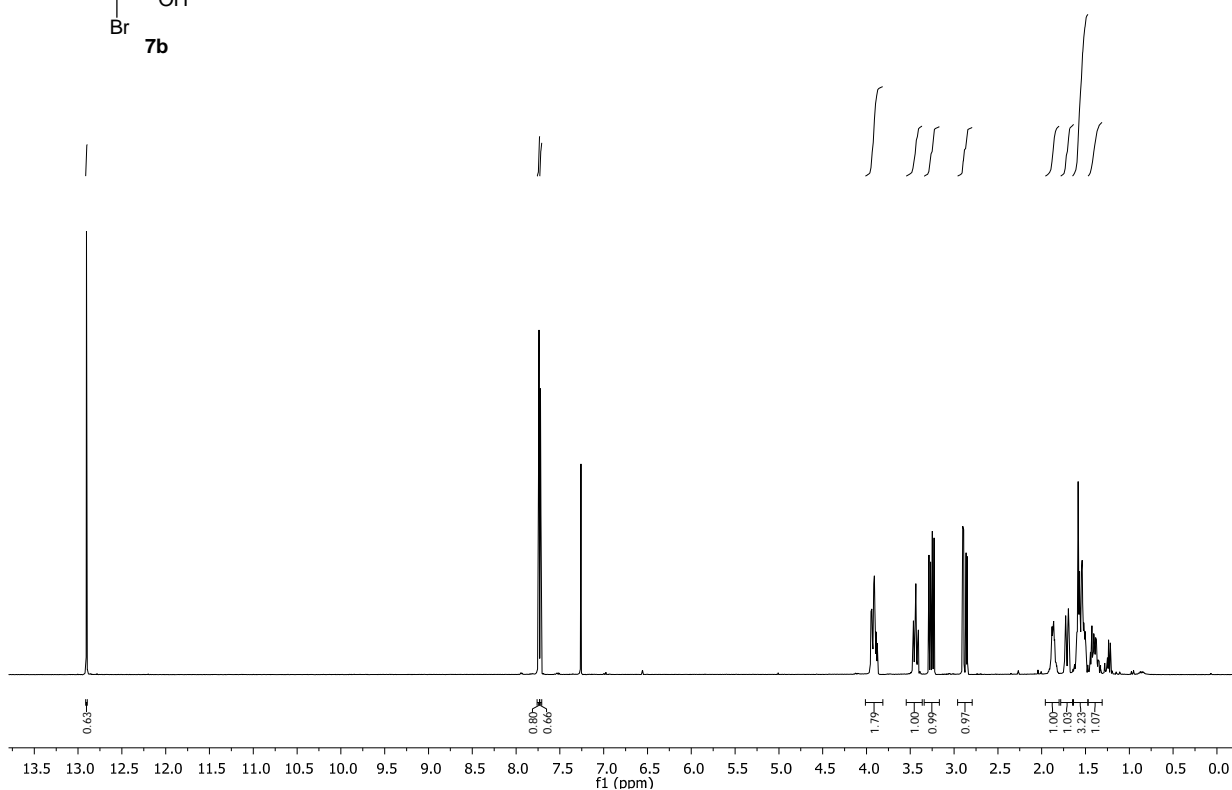
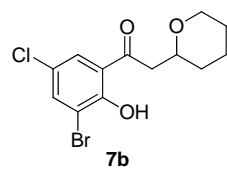


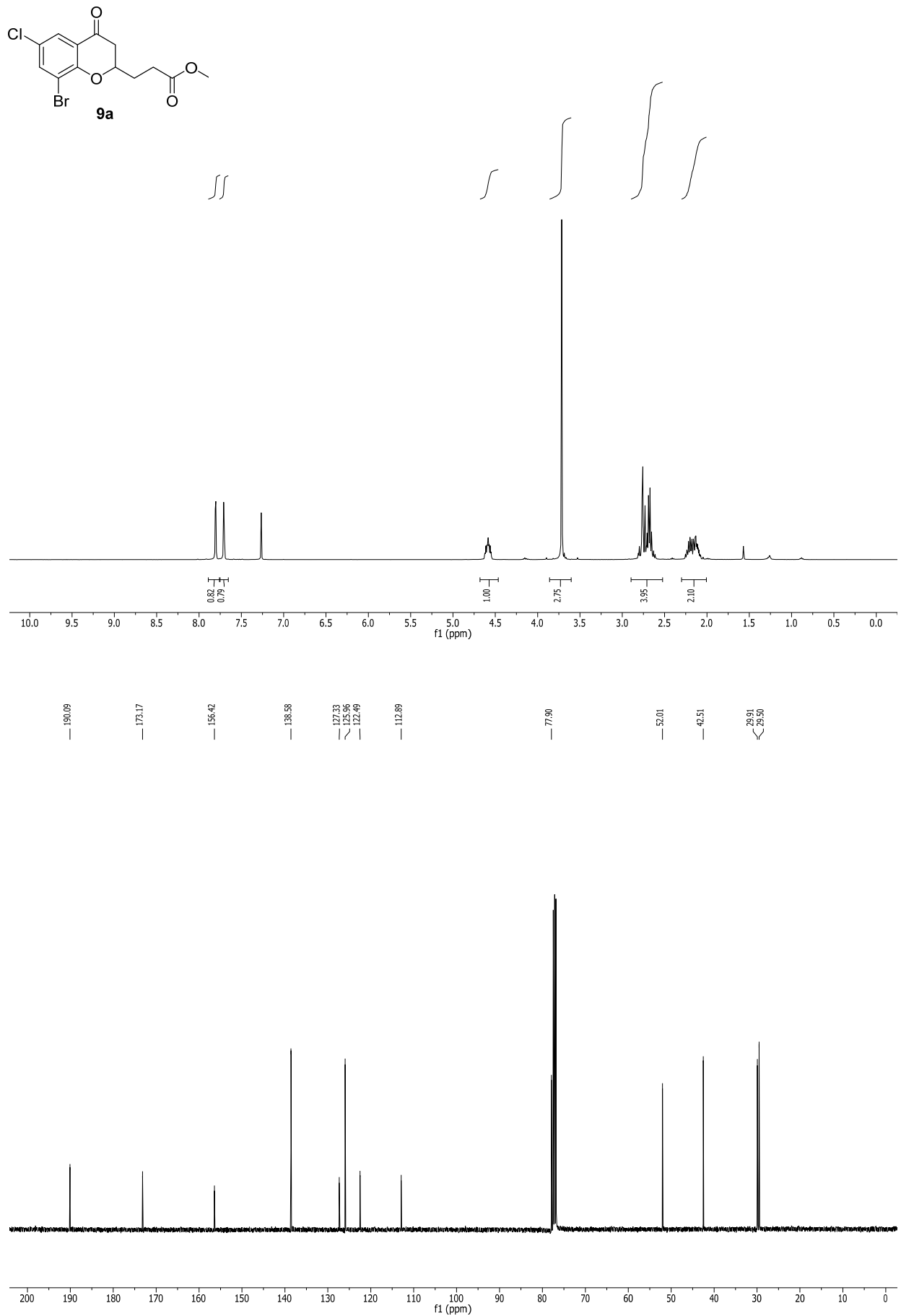


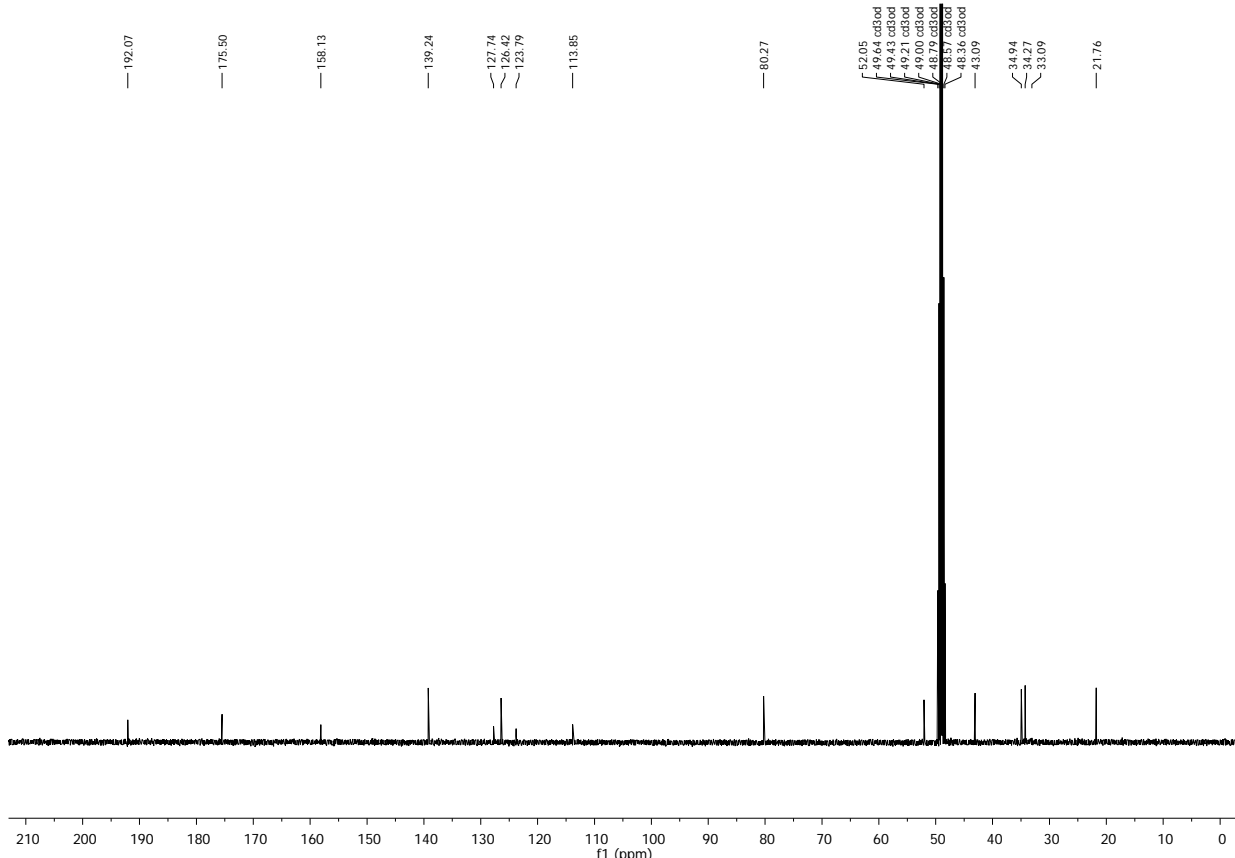
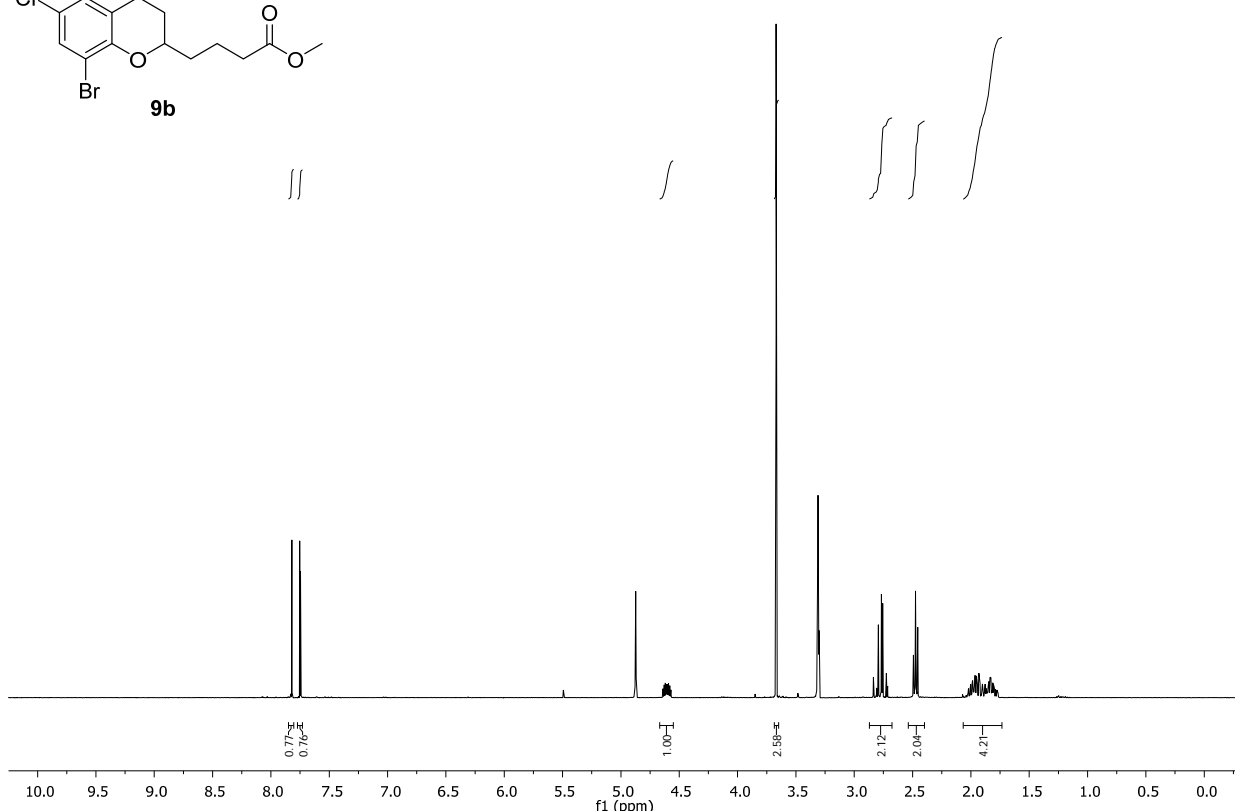
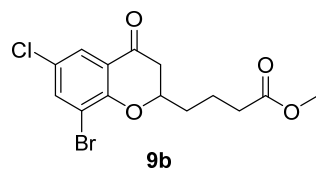


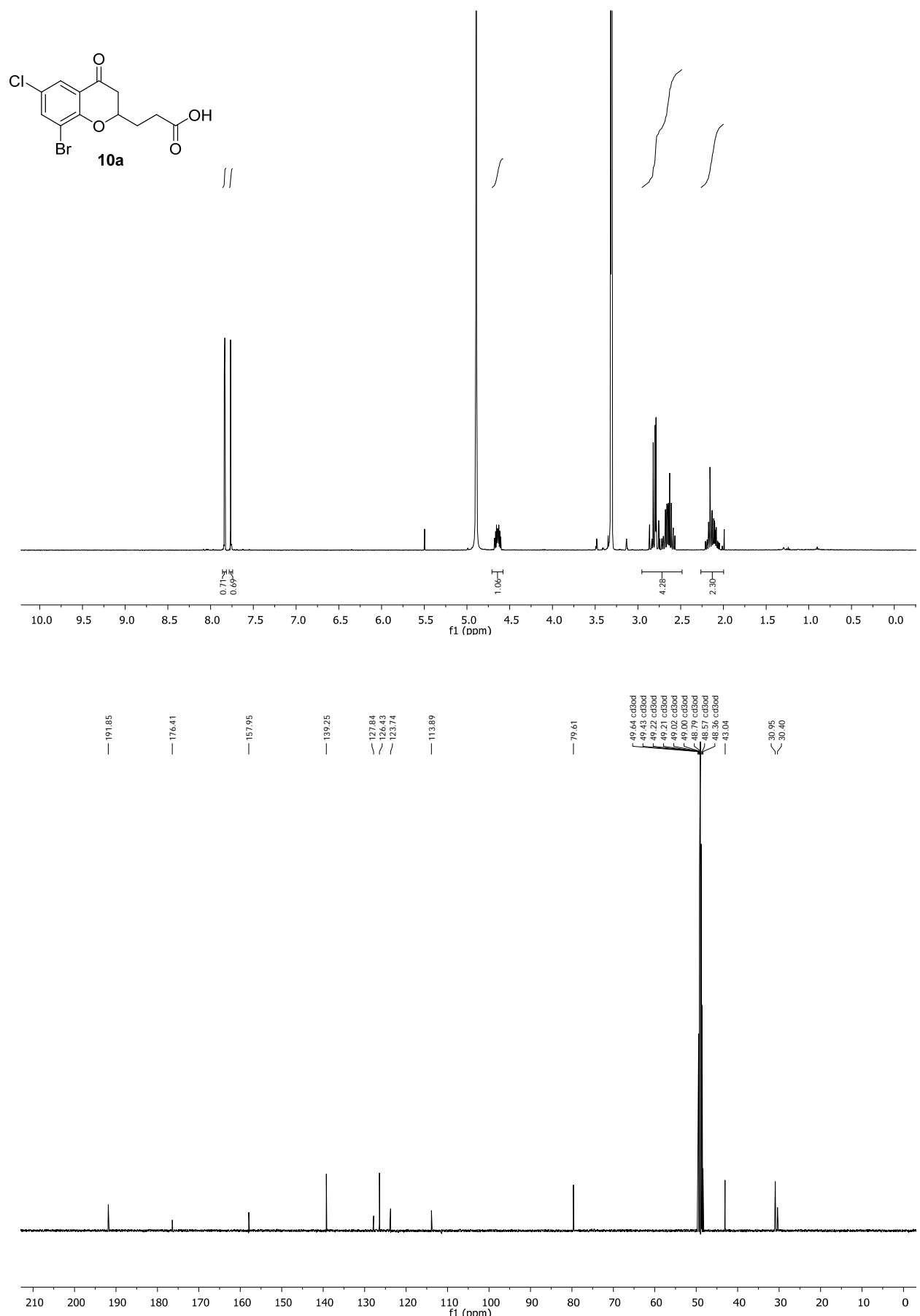


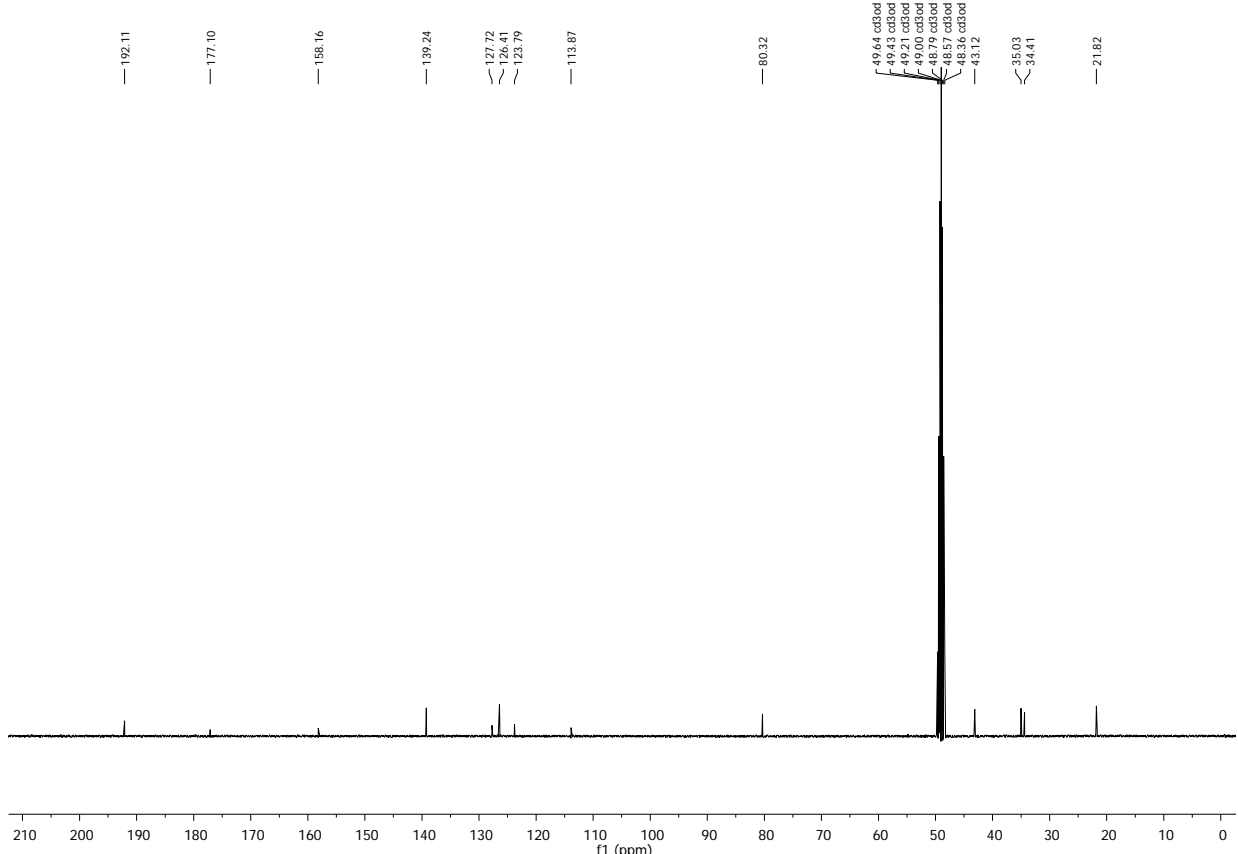
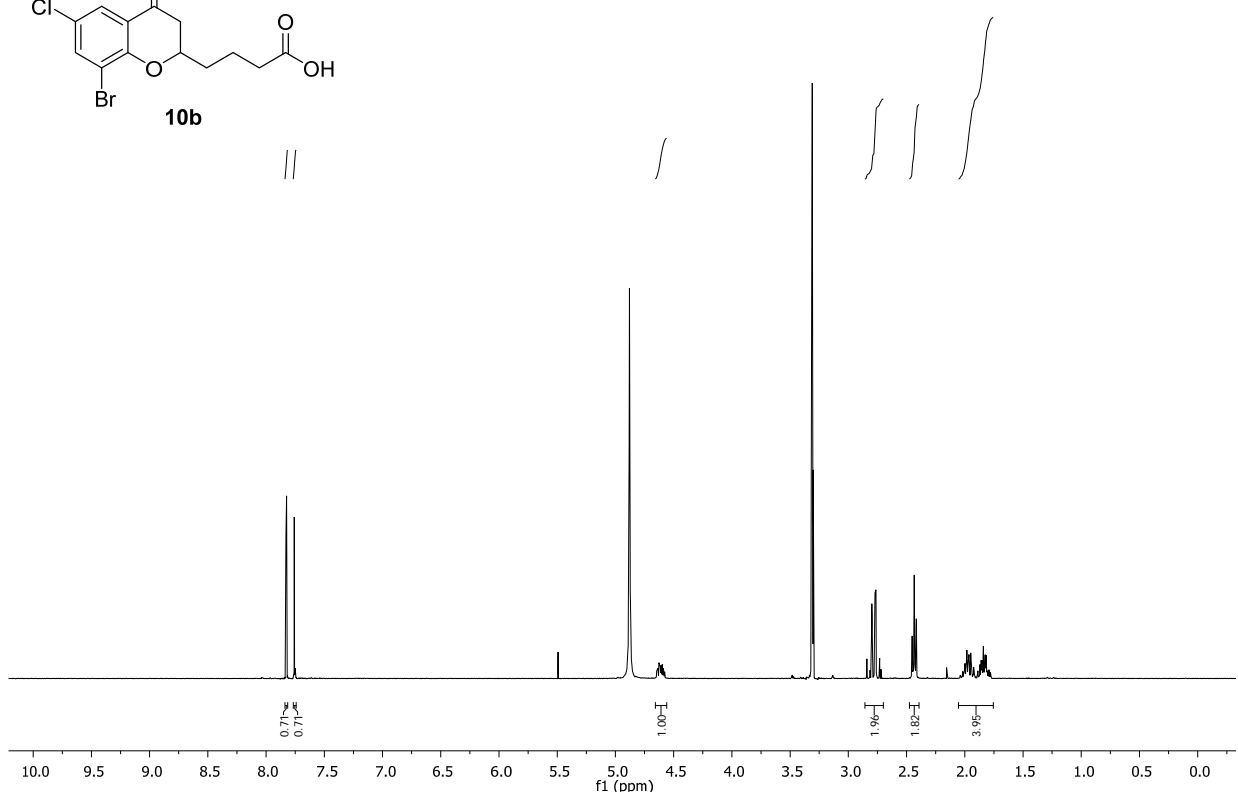
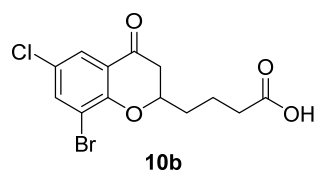


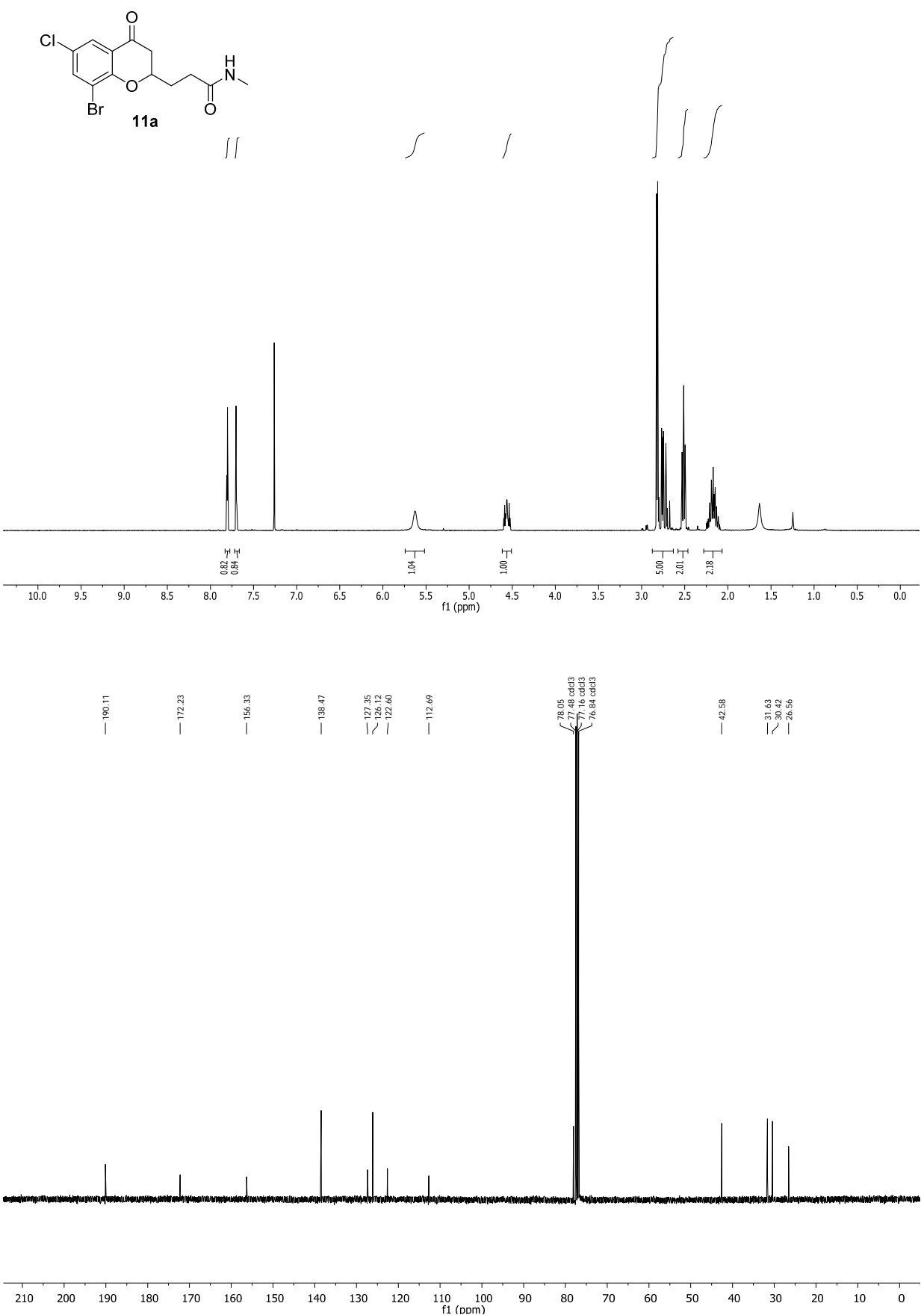


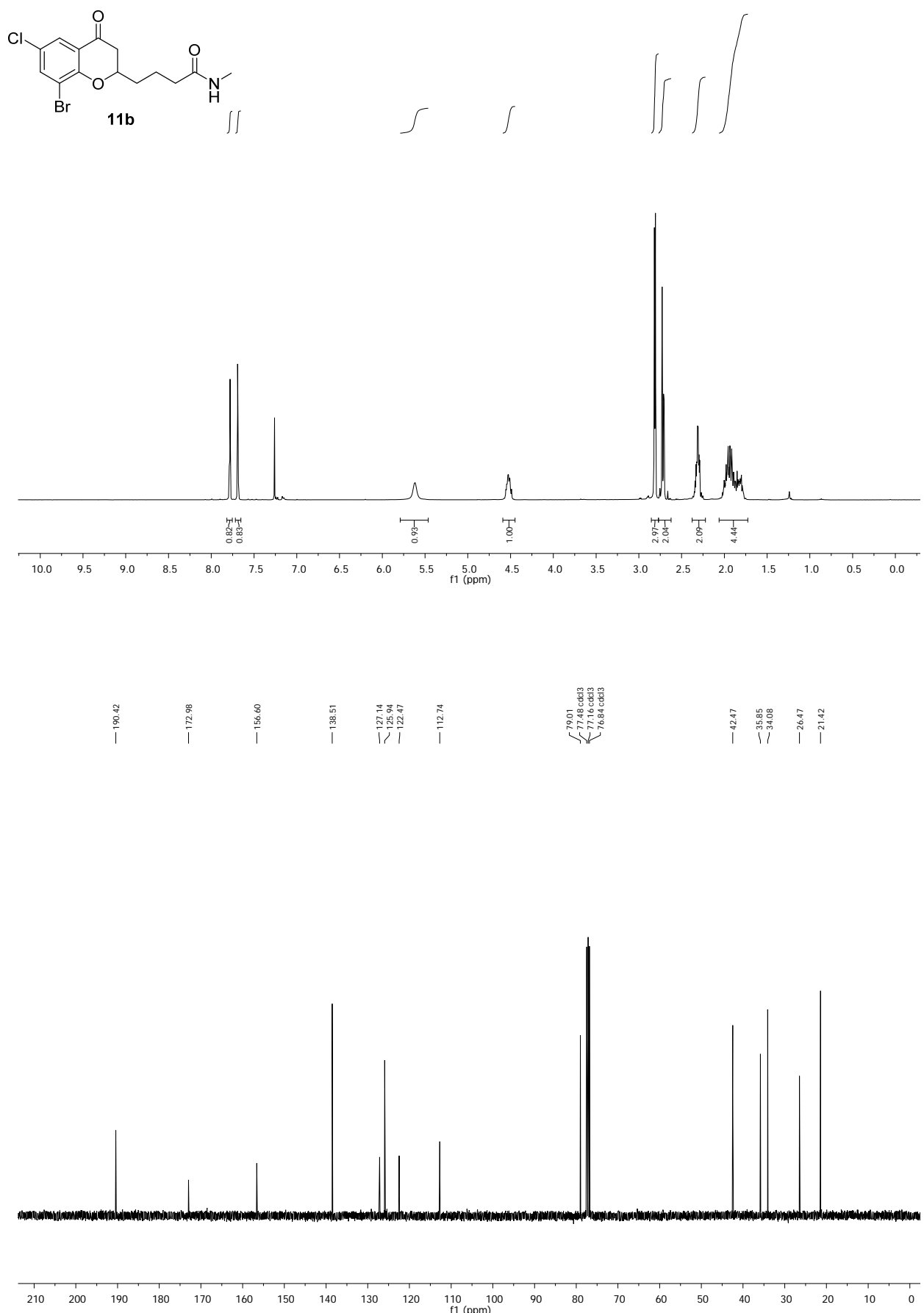


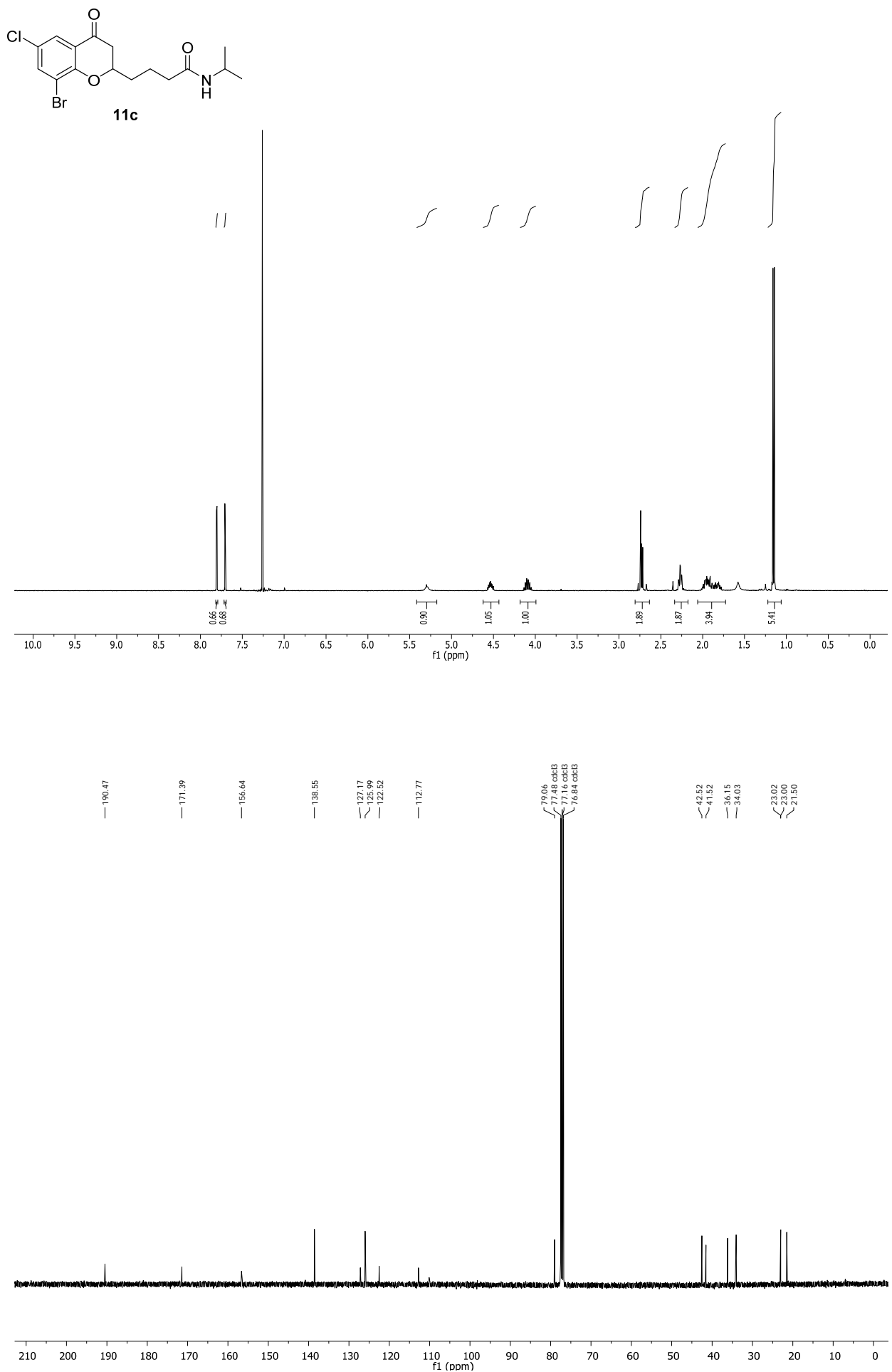


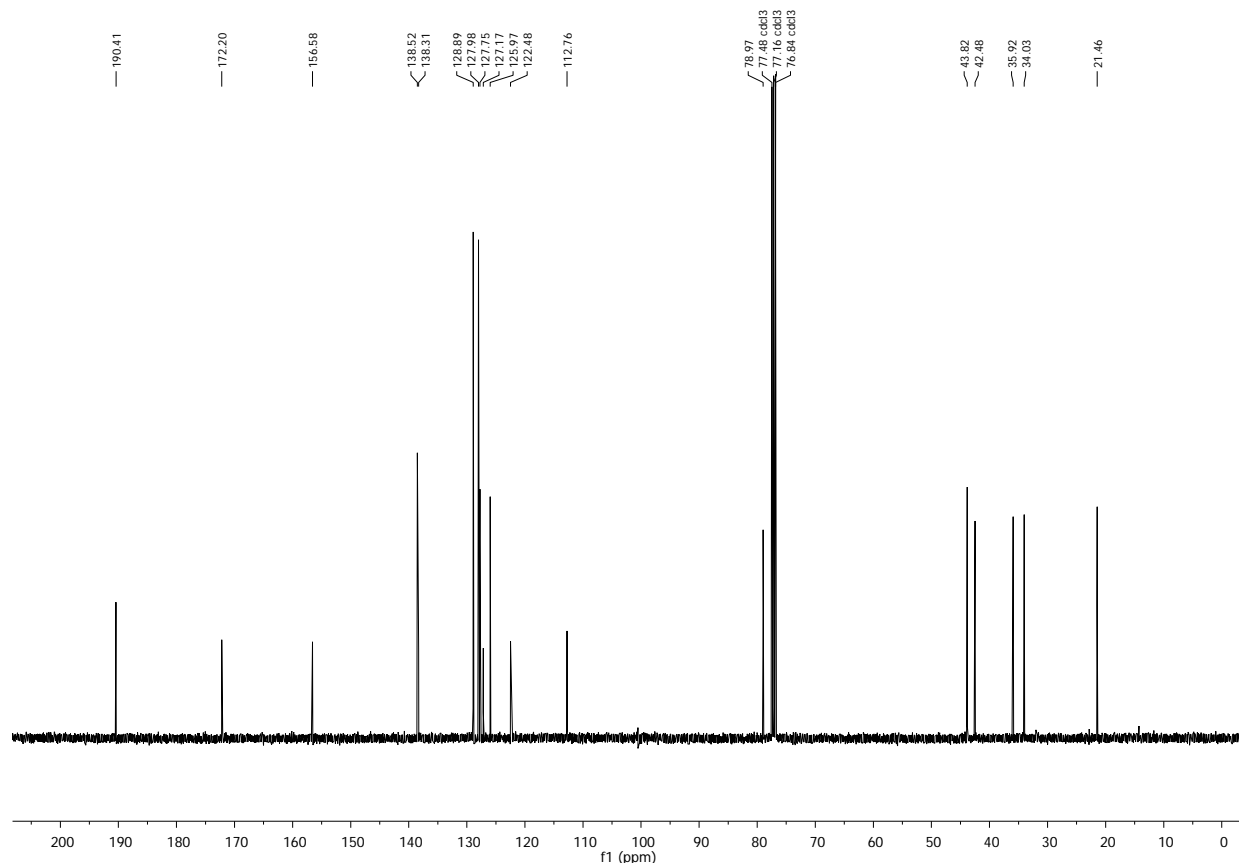
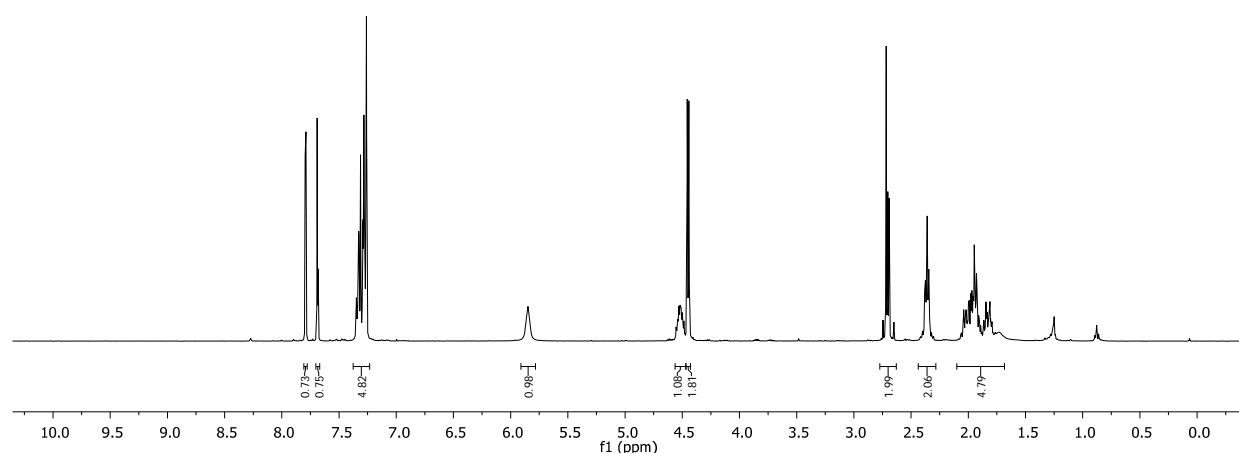
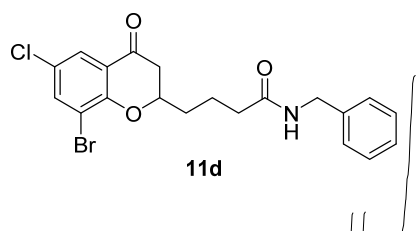


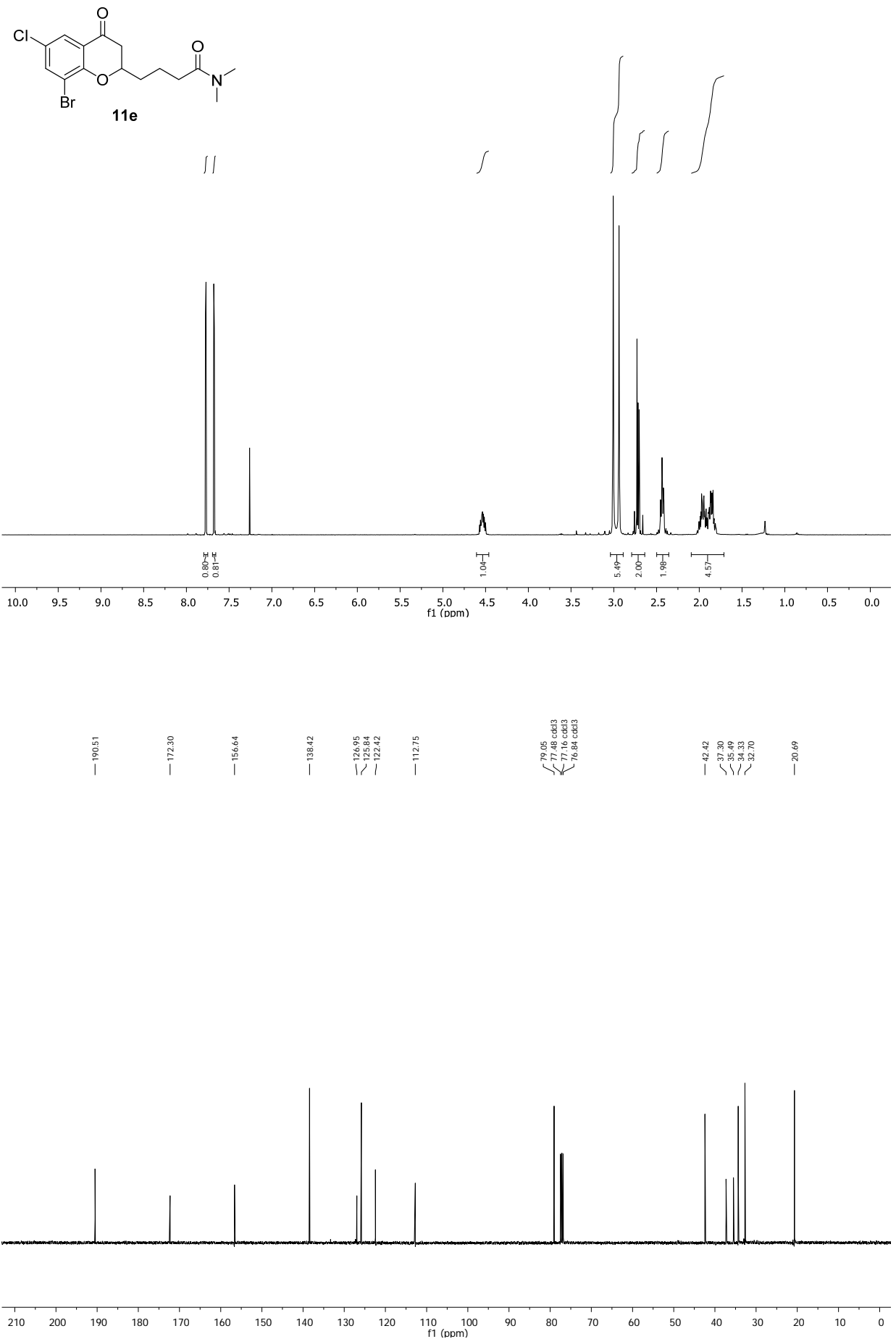


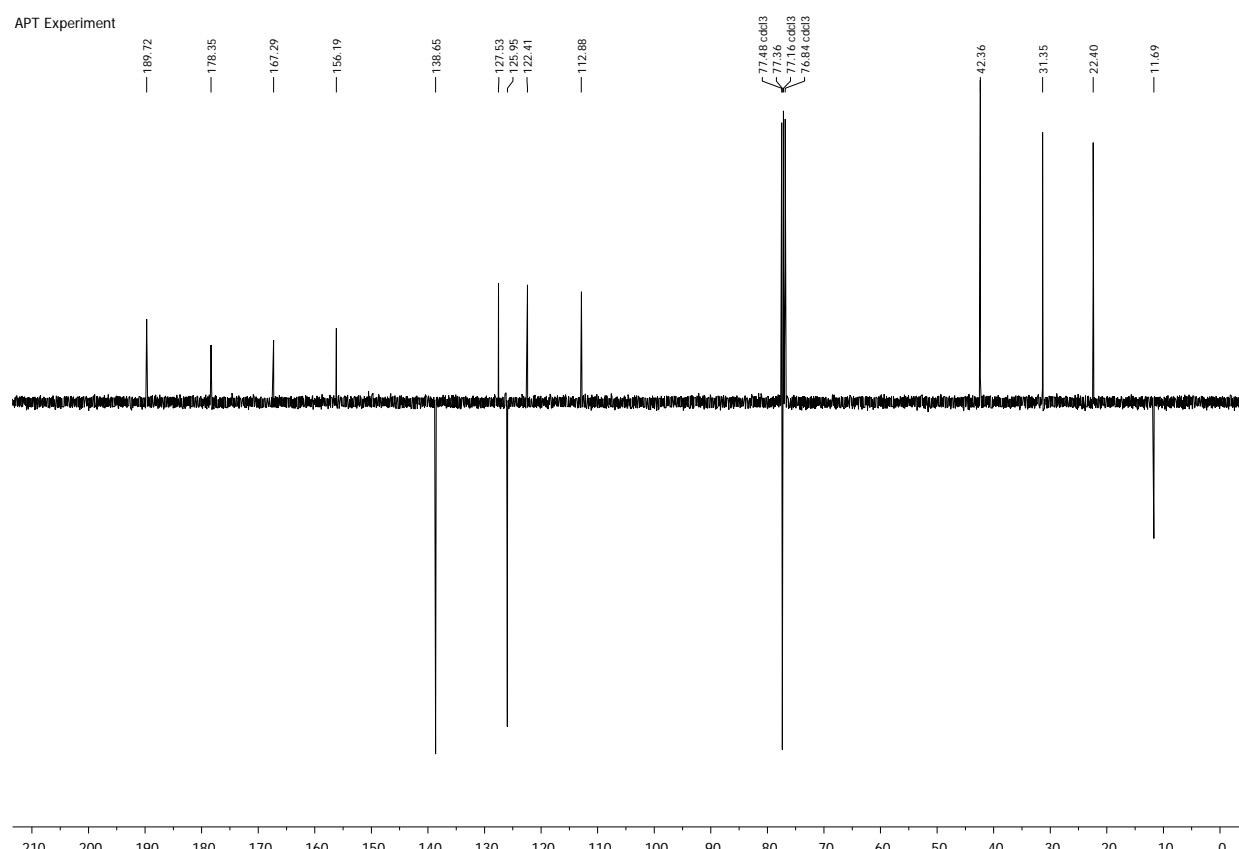
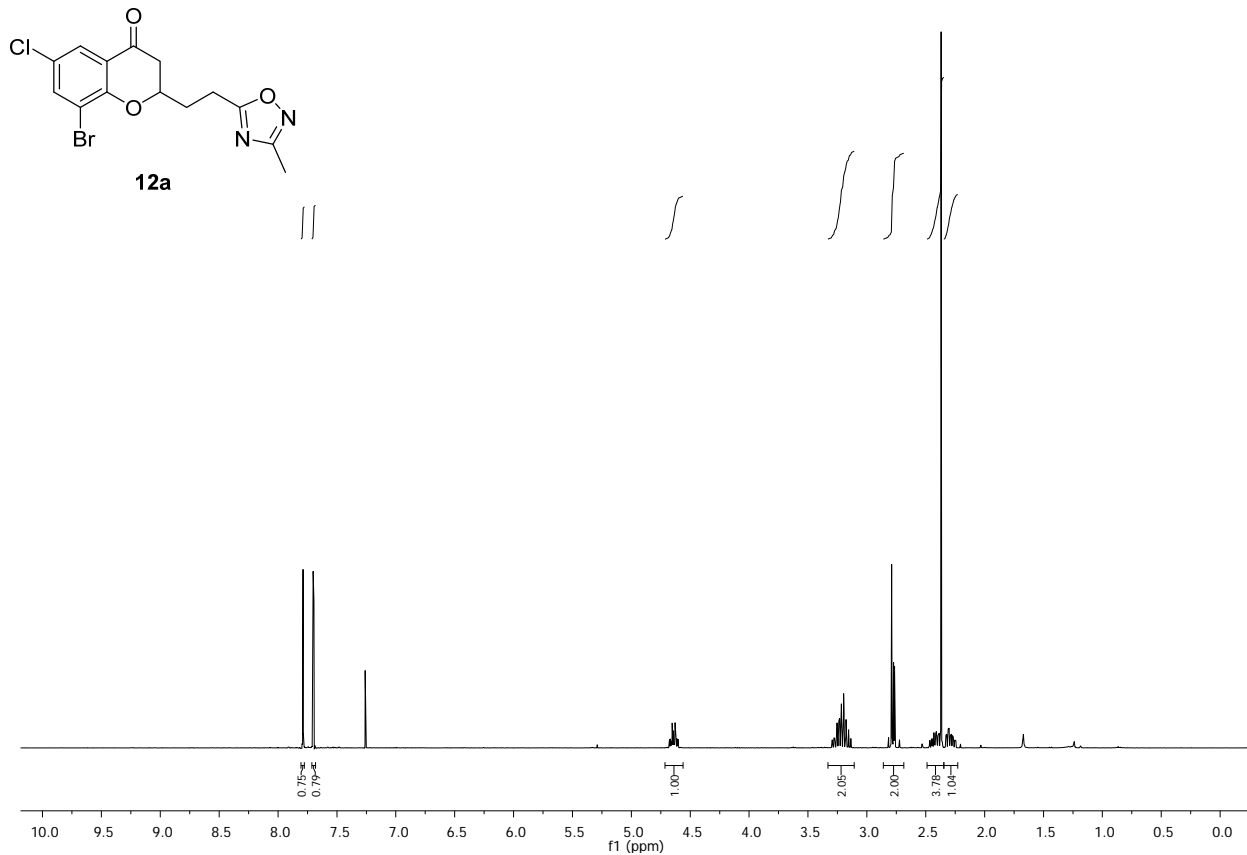


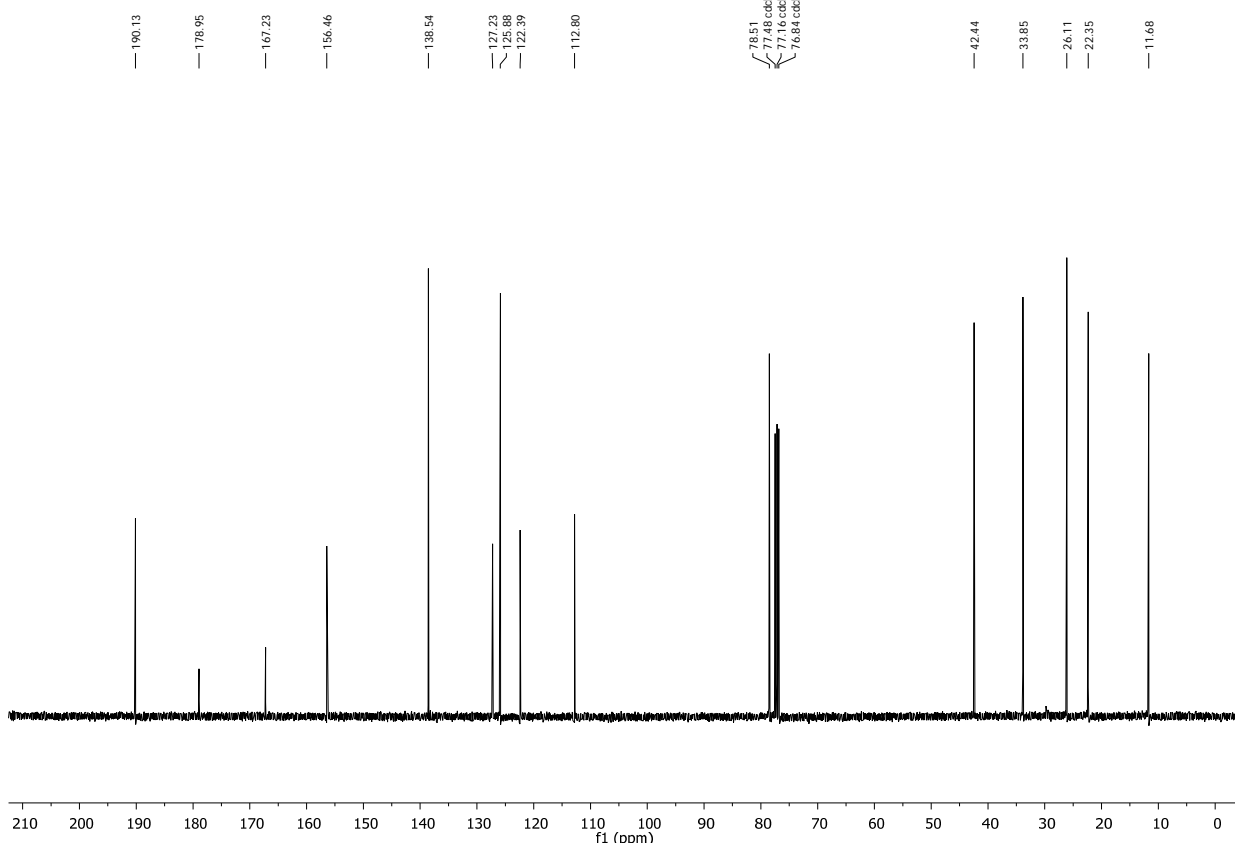
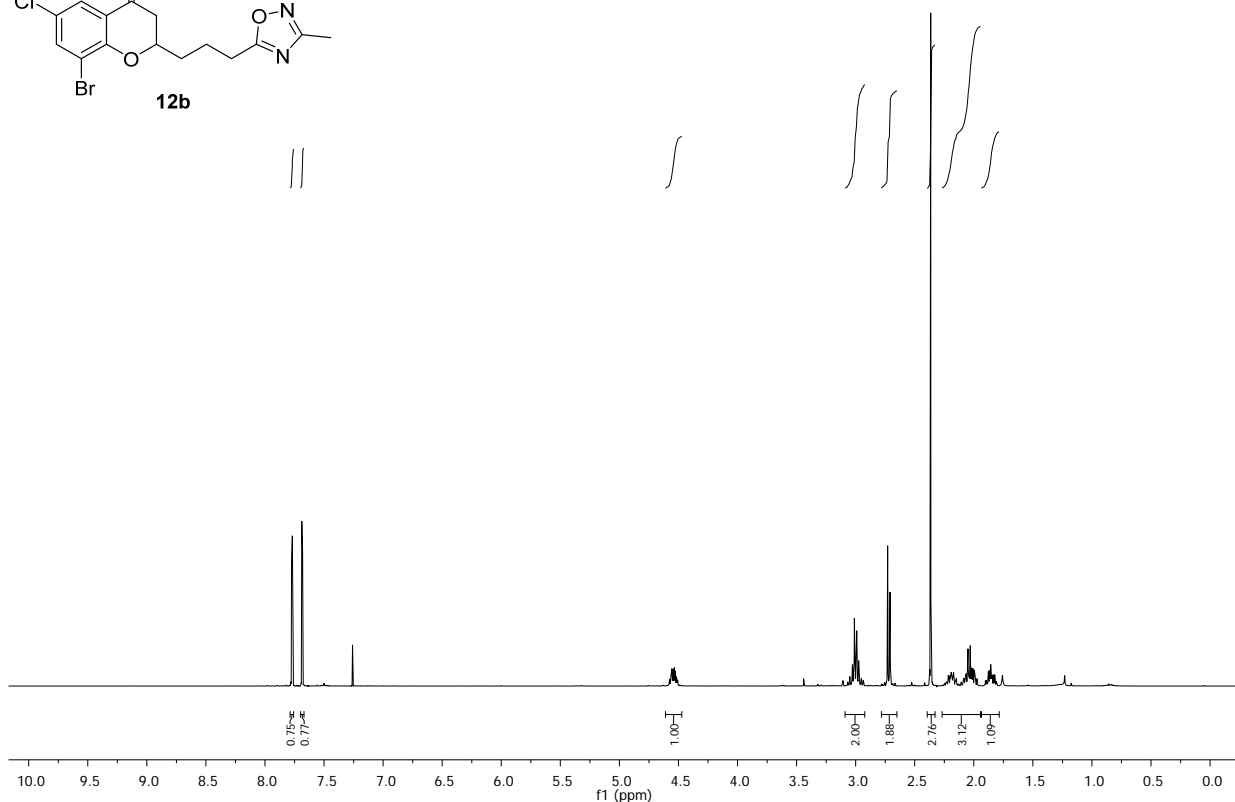
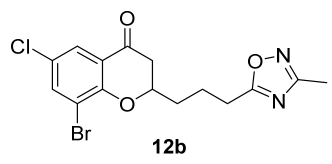


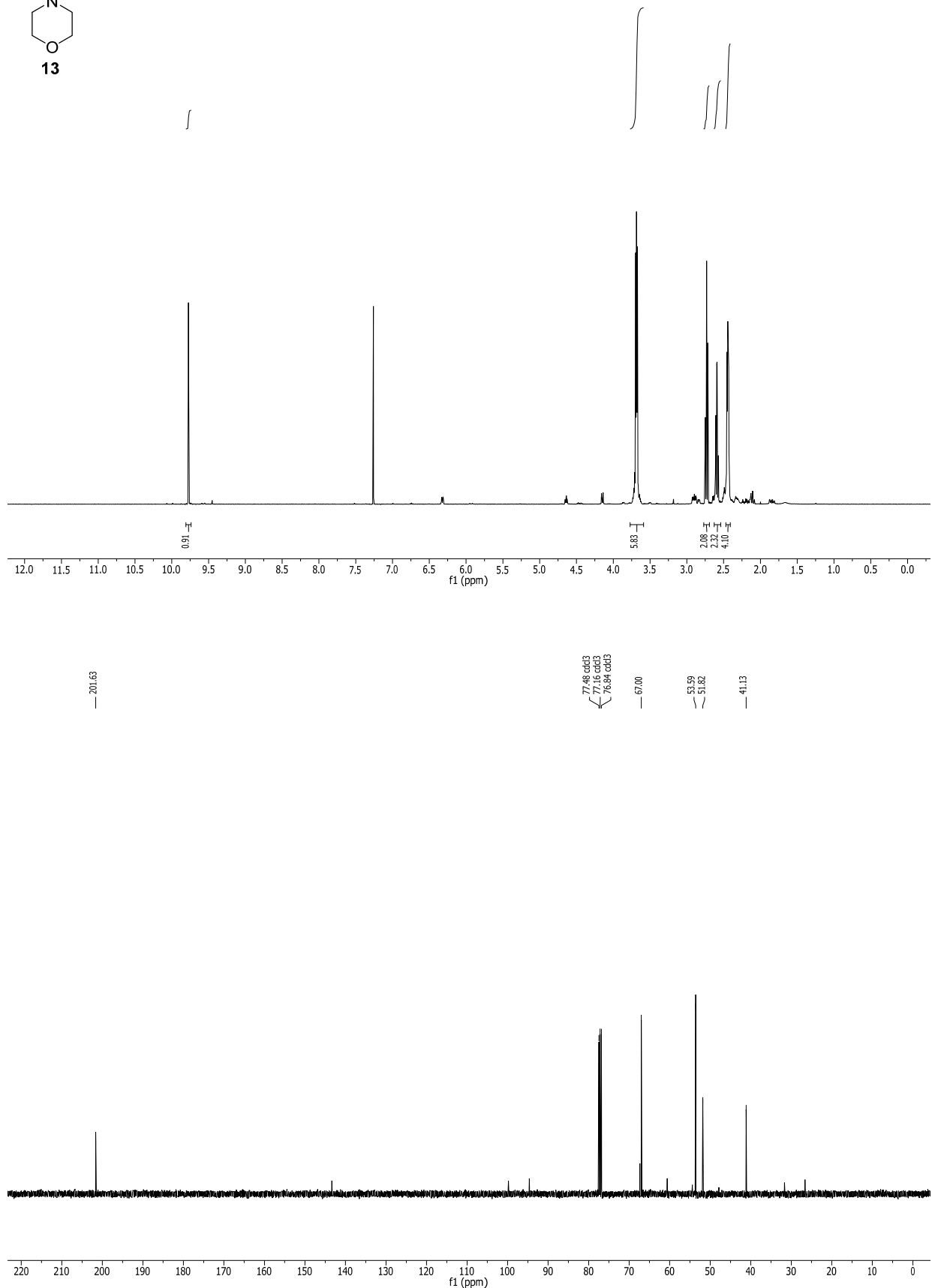
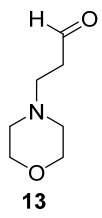


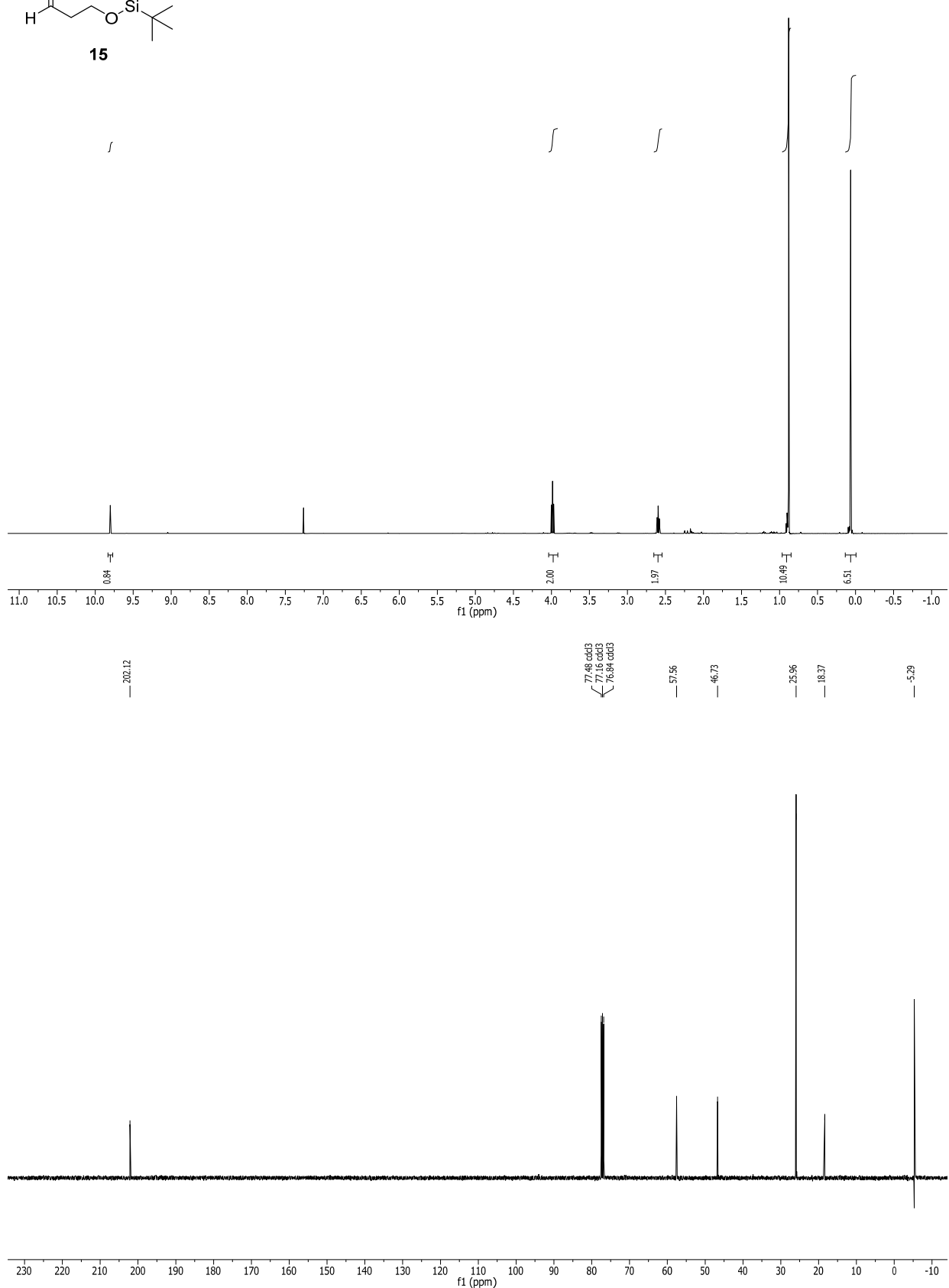
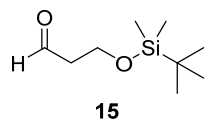


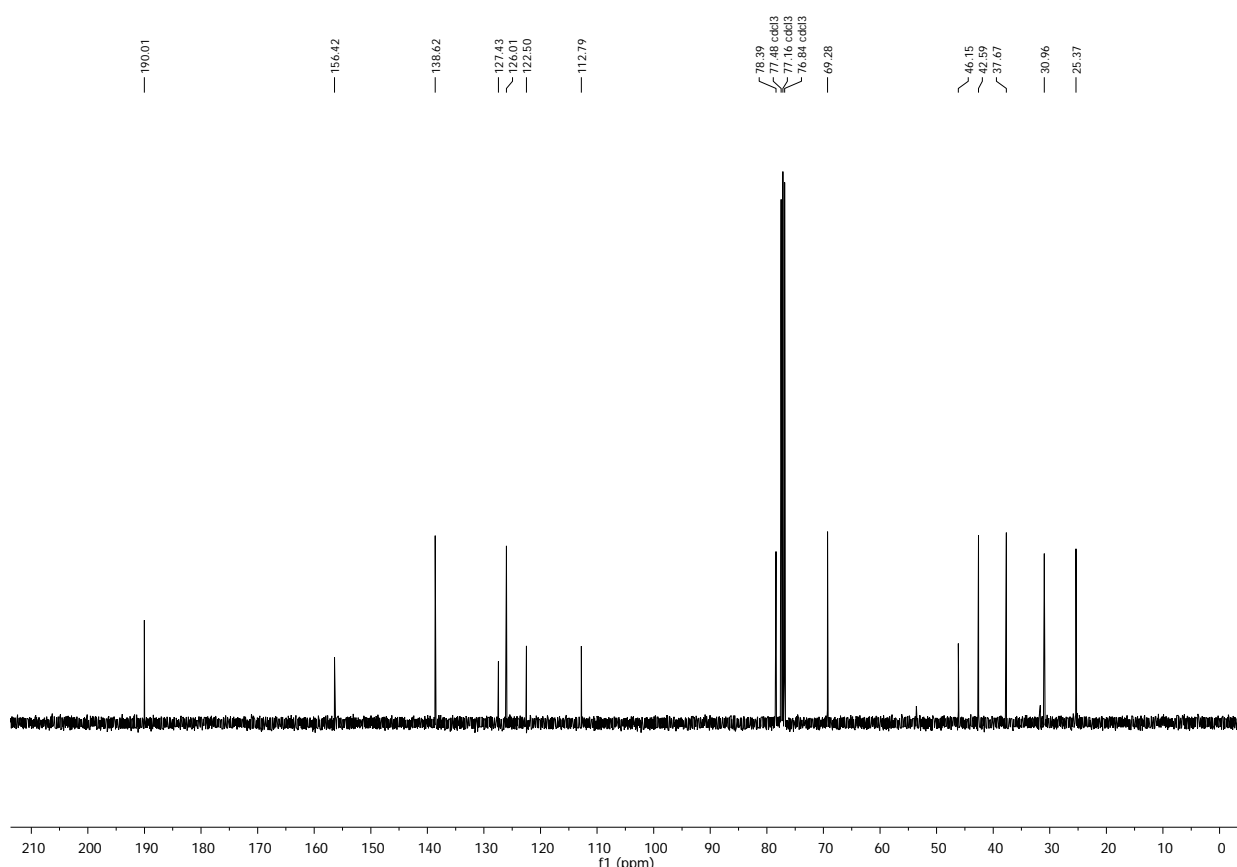
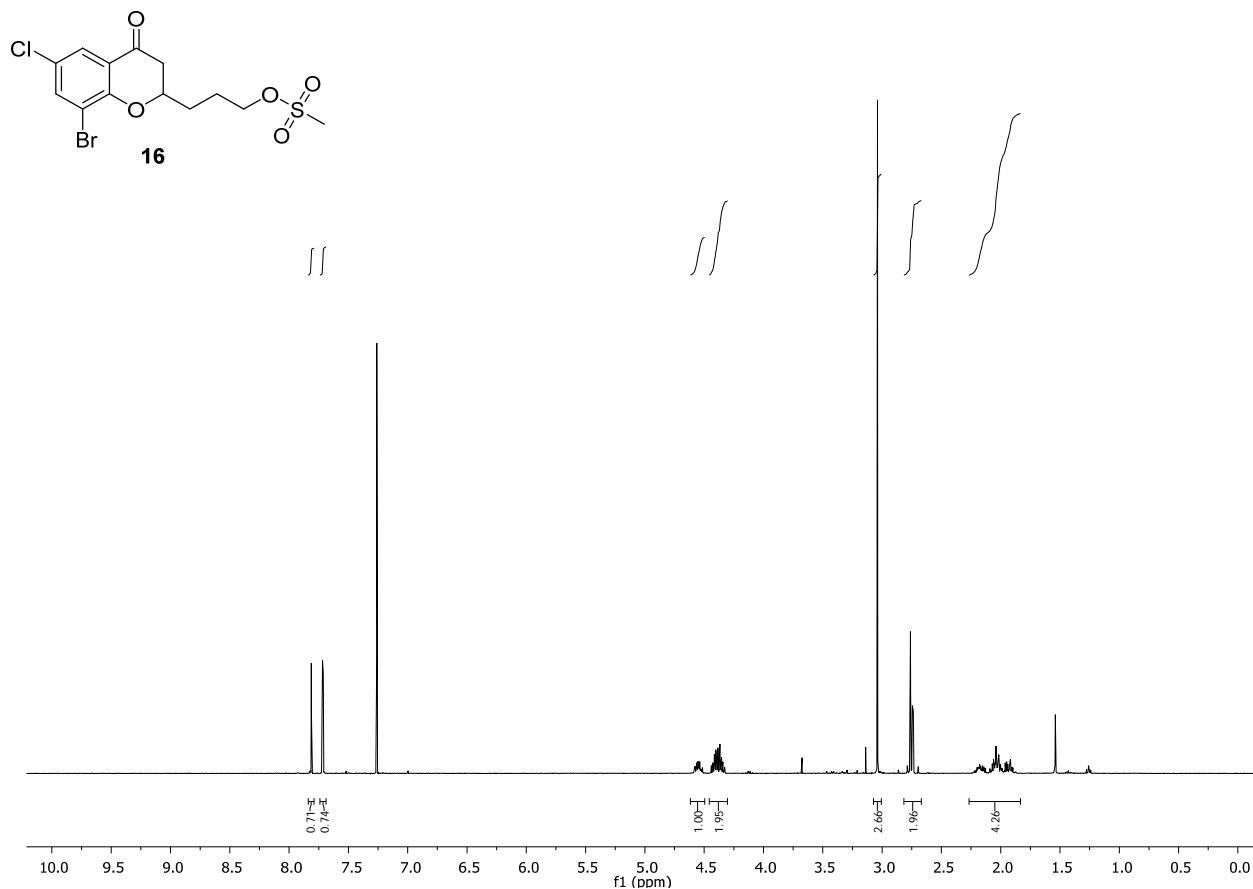


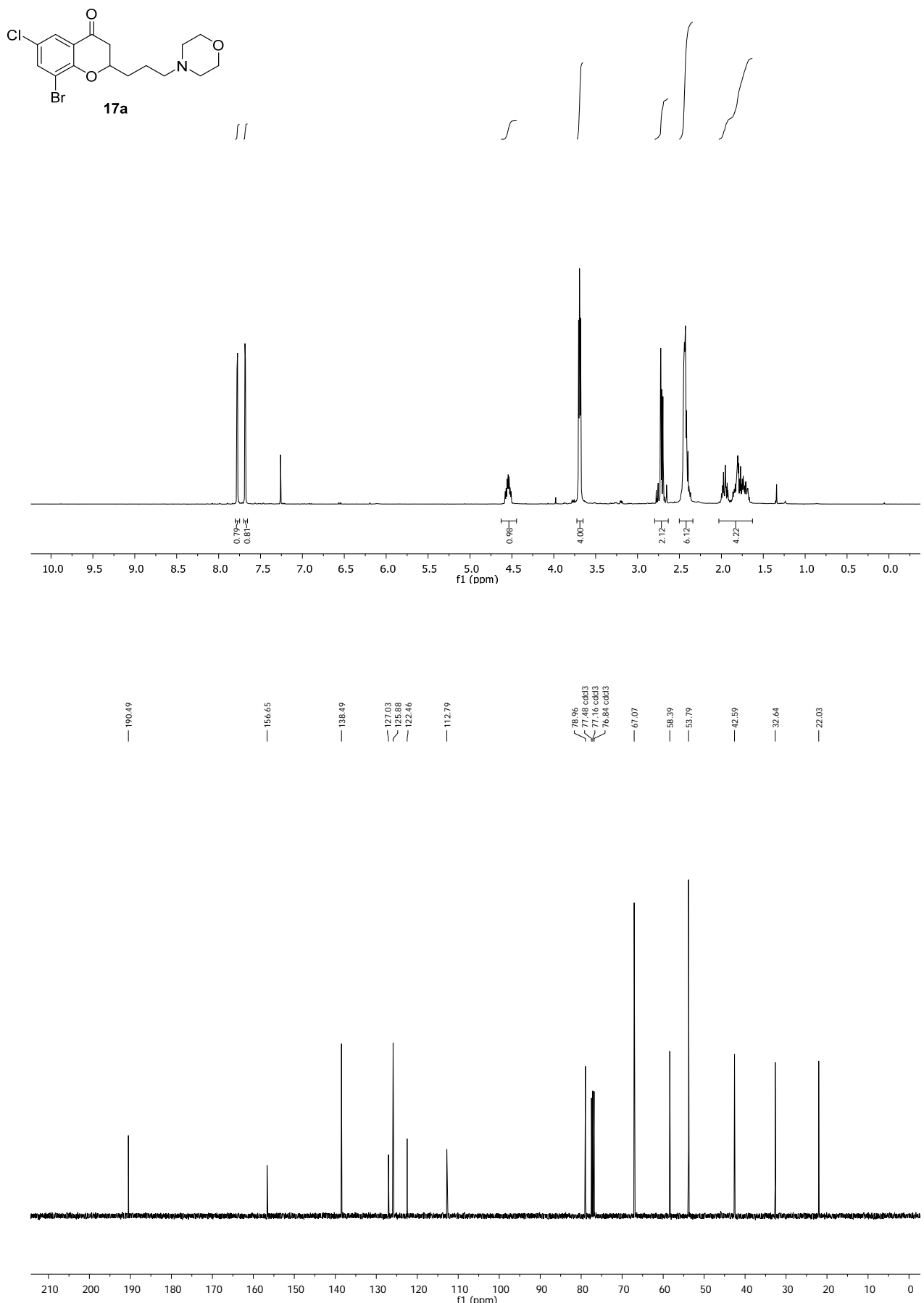


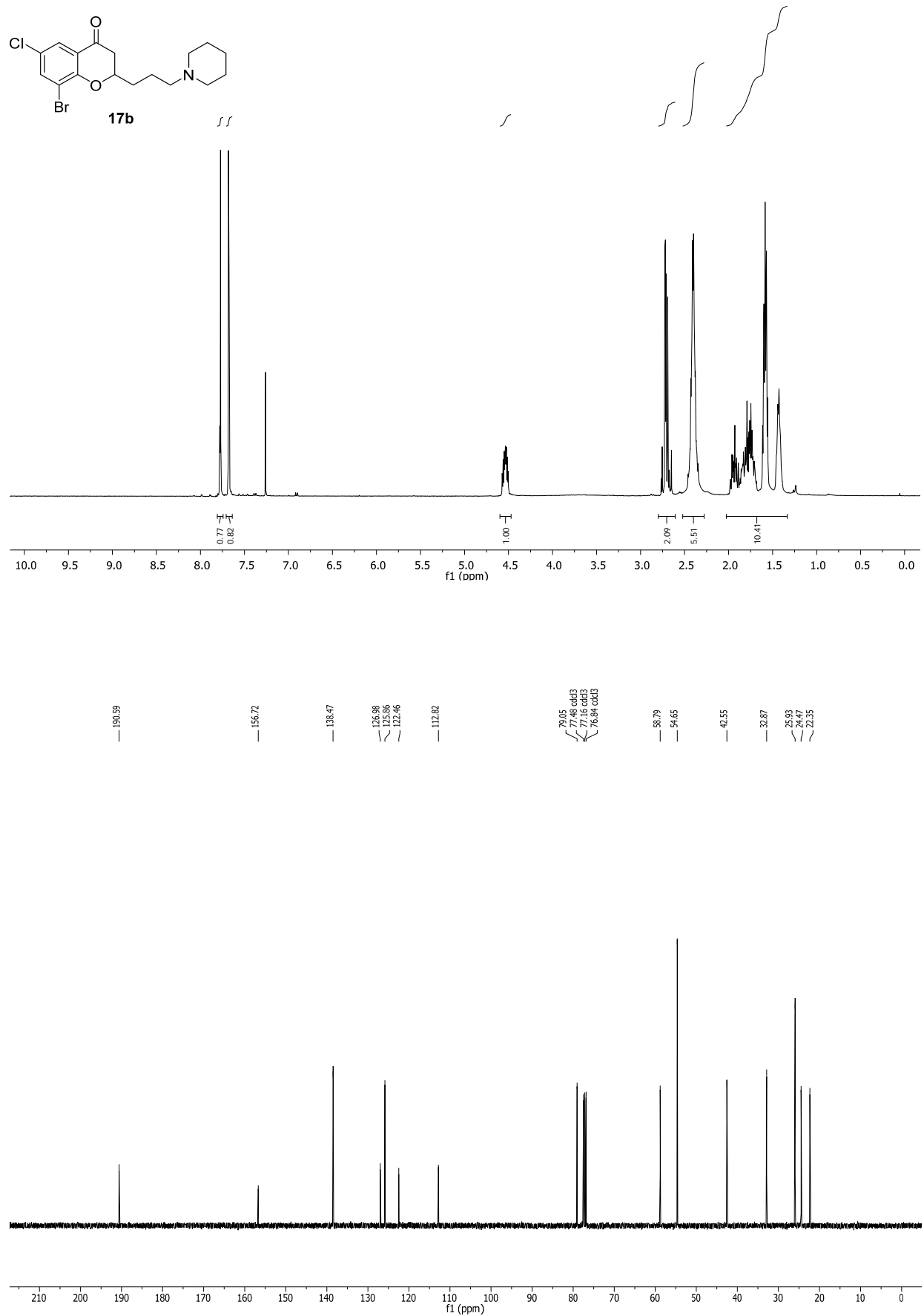


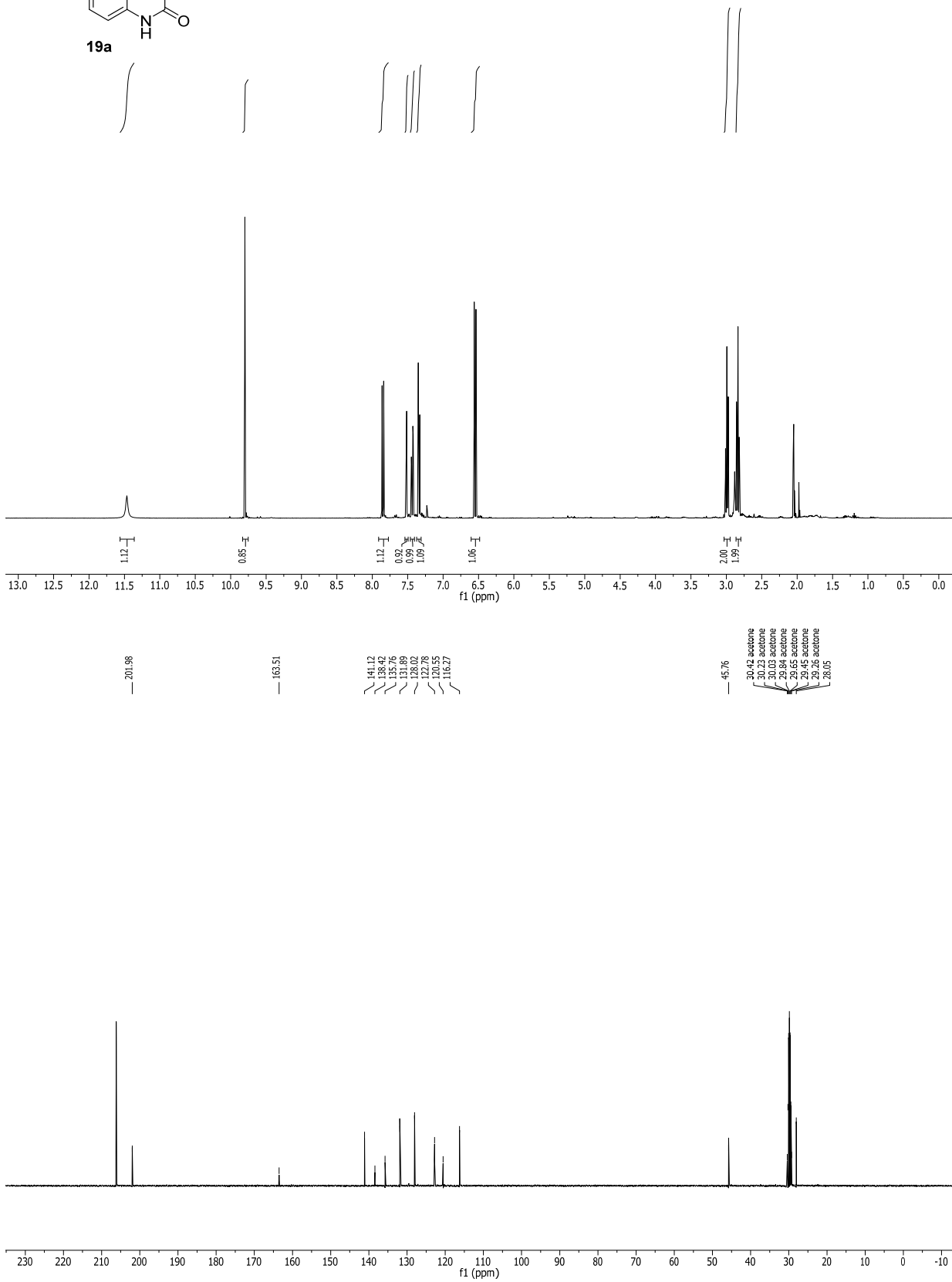
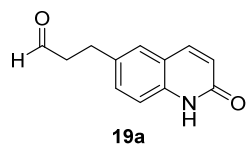


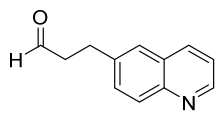




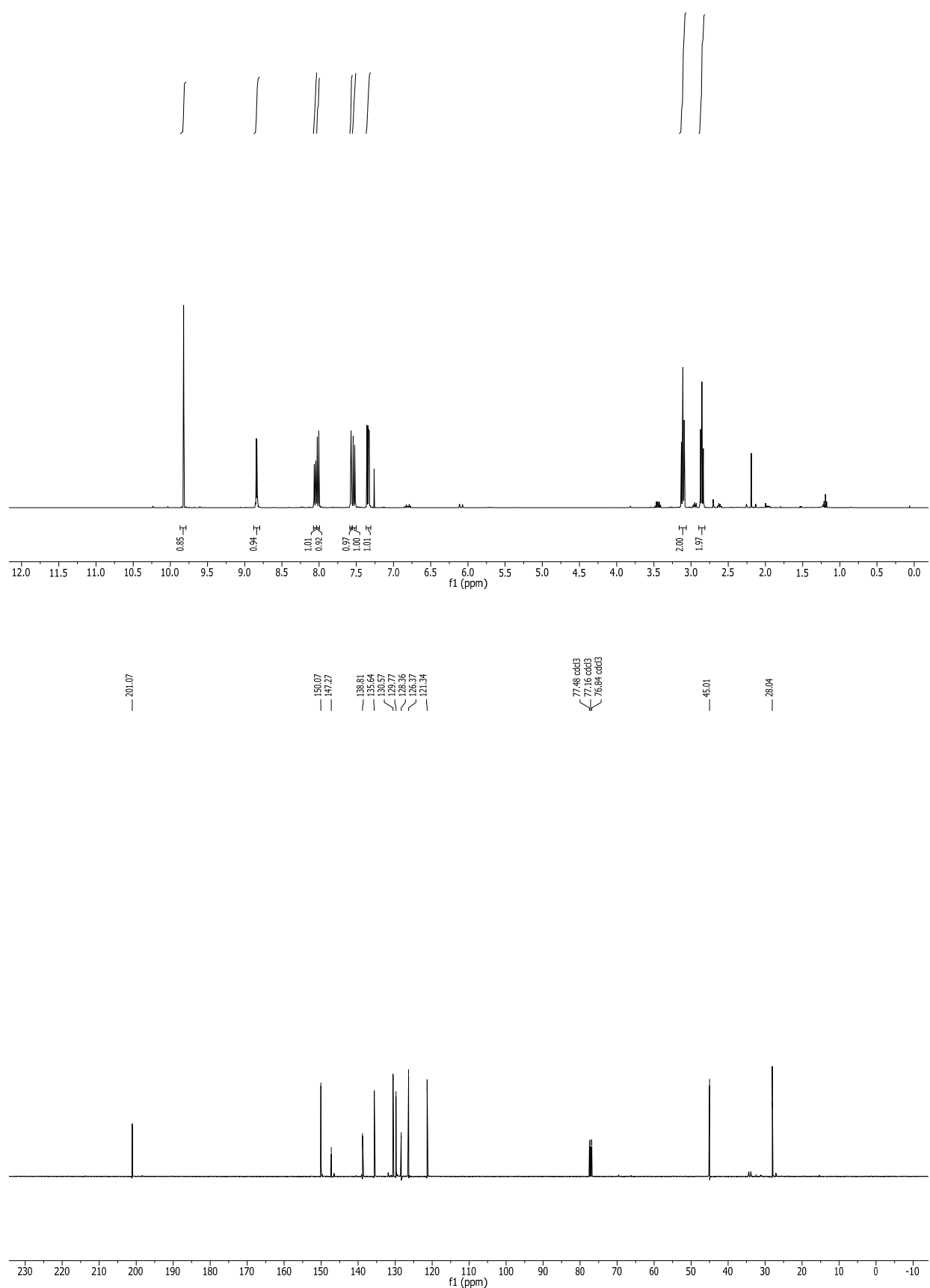


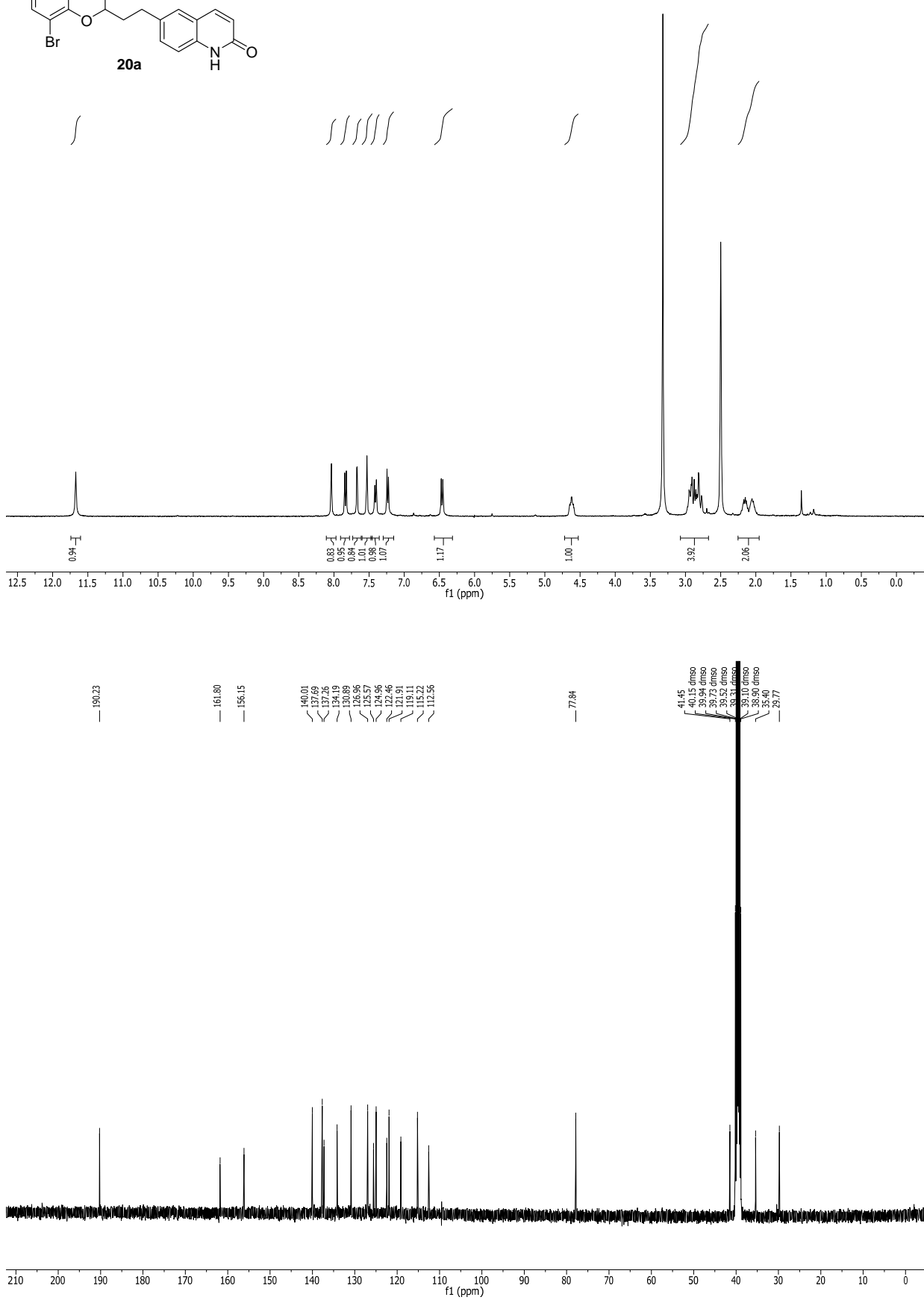
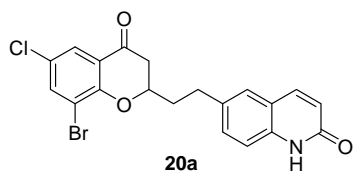


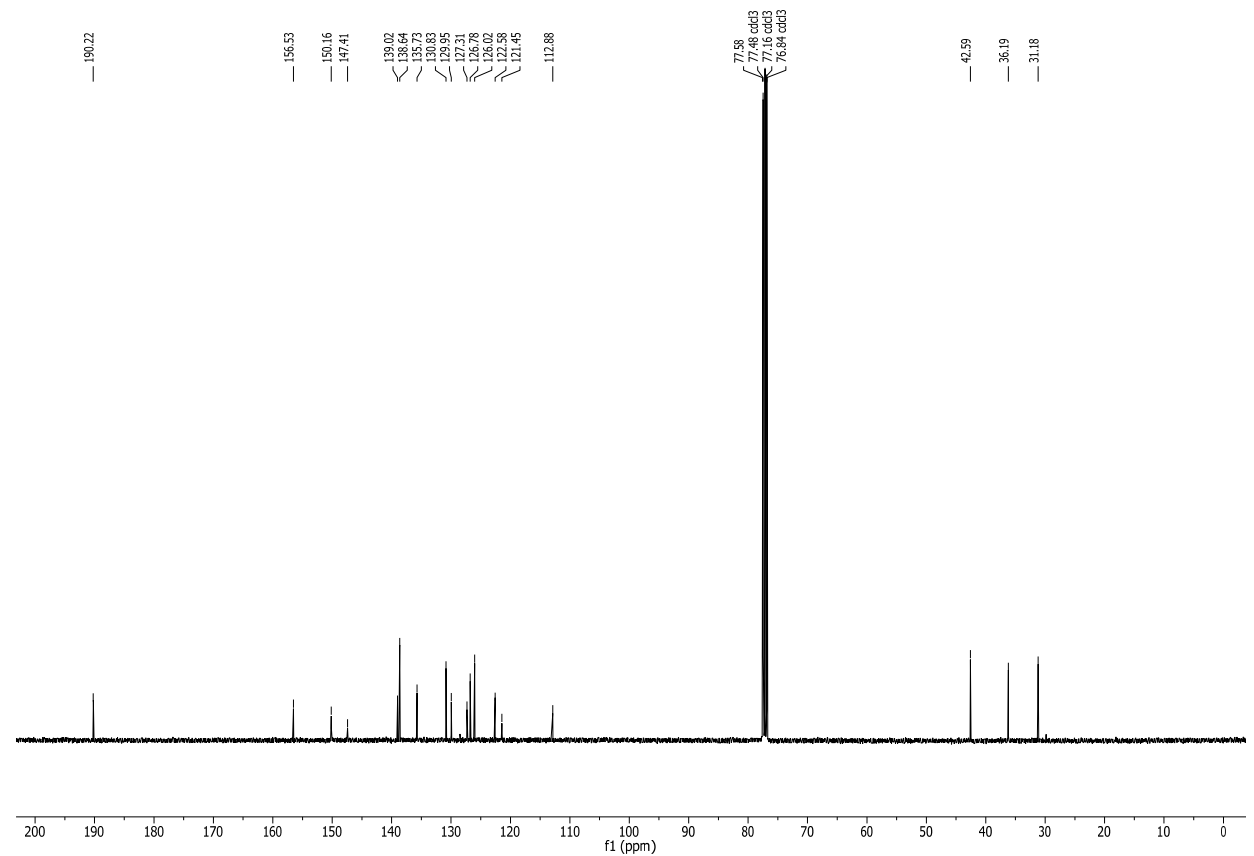
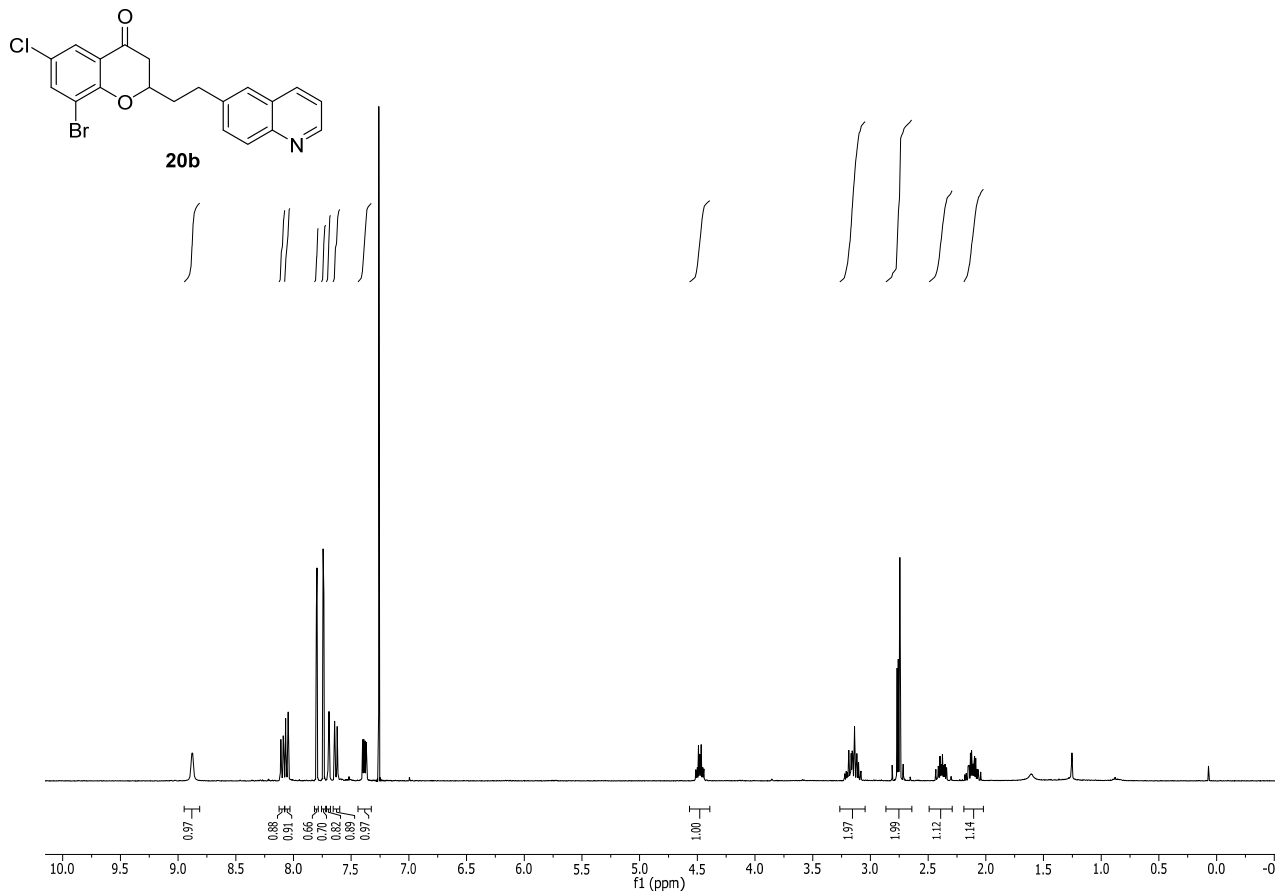


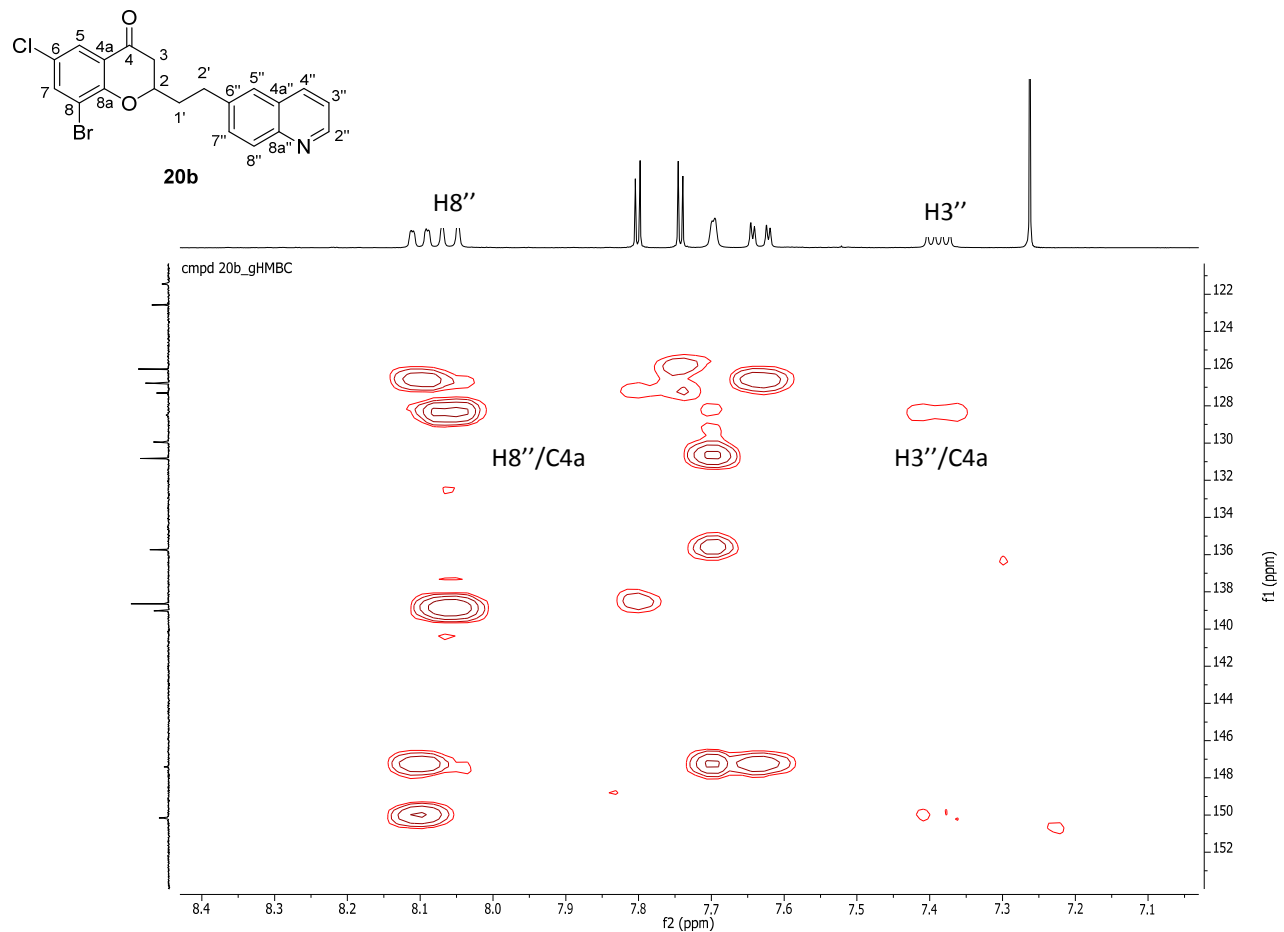


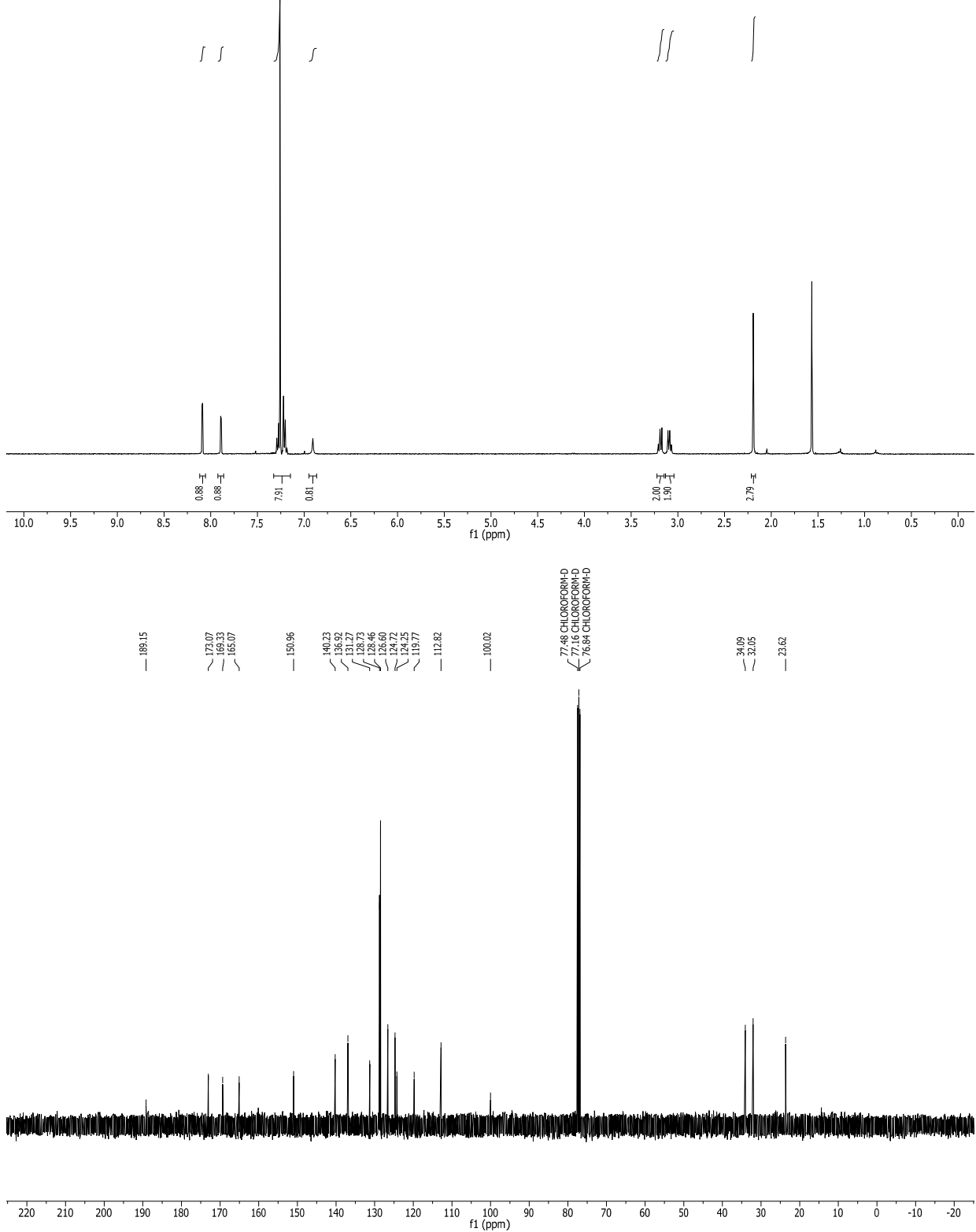
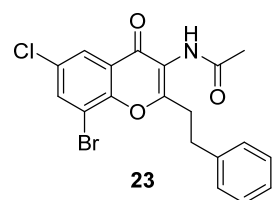
**19b**

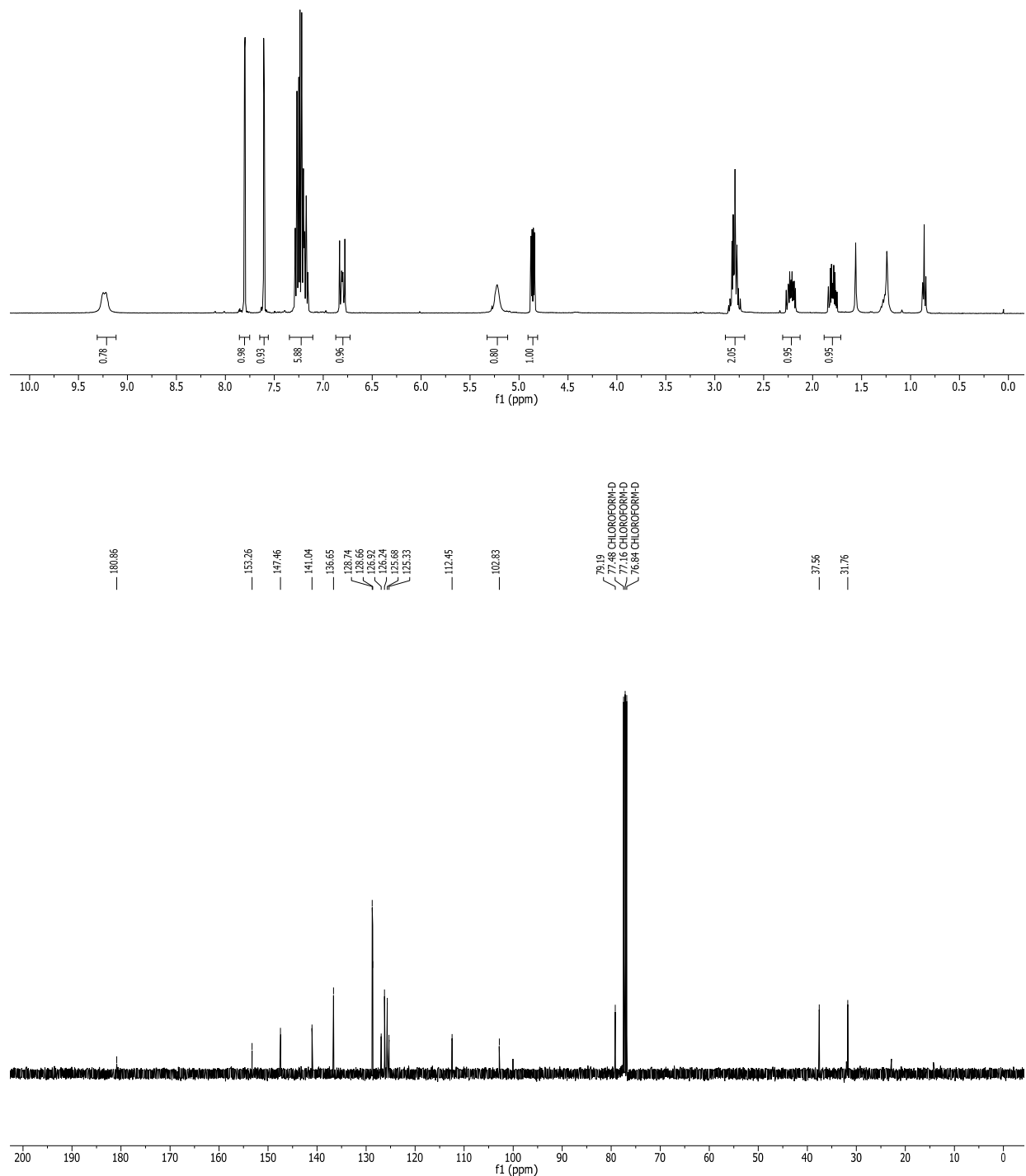
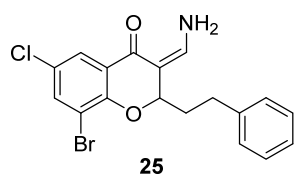












## 7 References

- (1) Zhao, X.; Allison, D.; Condon, B.; Zhang, F. Y.; Gheyi, T.; Zhang, A. P.; Ashok, S.; Russell, M.; MacEwan, I.; Qian, Y. W.; Jamison, J. A.; Luz, J. G. The 2.5 Å Crystal Structure of the SIRT1 Catalytic Domain Bound to Nicotinamide Adenine Dinucleotide (NAD(+)) and an Indole (EX527 Analogue) Reveals a Novel Mechanism of Histone Deacetylase Inhibition. *J. Med. Chem.* **2013**, *56*, 963-969.
- (2) Thompson, J. D.; Higgins, D. G.; Gibson, T. J. Clustal-W - Improving the Sensitivity of Progressive Multiple Sequence Alignment through Sequence Weighting, Position-Specific Gap Penalties and Weight Matrix Choice. *Nucleic Acids Res.* **1994**, *22*, 4673-4680.
- (3) Berman, H. M.; Westbrook, J.; Feng, Z.; Gilliland, G.; Bhat, T. N.; Weissig, H.; Shindyalov, I. N.; Bourne, P. E. The Protein Data Bank. *Nucleic Acids Res.* **2000**, *28*, 235-242.
- (4) Fechteler, T.; Dengler, U.; Schomburg, D. Prediction of protein three-dimensional structures in insertion and deletion regions: a procedure for searching data bases of representative protein fragments using geometric scoring criteria. *J. Mol. Biol.* **1995**, *253*, 114-131.
- (5) Labute, P. Protonate3D: Assignment of ionization states and hydrogen coordinates to macromolecular structures. *Proteins: Struct., Funct., Bioinf.* **2009**, *75*, 187-205.
- (6) Hoff, K. G.; Avalos, J. L.; Sens, K.; Wolberger, C. Insights into the sirtuin mechanism from ternary complexes containing NAD(+) and acetylated peptide. *Structure* **2006**, *14*, 1231-1240.
- (7) Avalos, J. L.; Boeke, J. D.; Wolberger, C. Structural basis for the mechanism and regulation of Sir2 enzymes. *Mol. Cell* **2004**, *13*, 639-648.
- (8) Gertz, M.; Fischer, F.; Nguyen, G. T.; Lakshminarasimhan, M.; Schutkowski, M.; Weyand, M.; Steegborn, C. Ex-527 inhibits Sirtuins by exploiting their unique NAD+-dependent deacetylation mechanism. *Proc. Natl. Acad. Sci. U. S. A.* **2013**, *110*, E2772-2781.